Mon. Not. R. Astron. Soc. **000**, 000–000 (0000) Printed 29 June 2006 (MN LaTeX style file v2.2)

A statistical study of pulsar timing irregularities using observations from Jodrell Bank Observatory

G. Hobbs,[1] A.G. Lyne,[2] M. Kramer[2]
[1] *Australia Telescope National Facility, CSIRO, PO Box 76, Epping NSW 1710, Australia*
[2] *University of Manchester, Jodrell Bank Observatory, Macclesfield, Cheshire SK11 9DL*

ABSTRACT

We provide an analysis of structures observed in the timing residuals of 374 pulsars. Observations obtained using the 76-m Lovell radio telescope over the last 20 years have allowed us to carry-out the first large-scale analysis of pulsar timing noise containing long-data spans, numerous observations at multiple frequencies for a large number of pulsars. We plot the timing residuals for each of these pulsars and carry out statistical analyses in order to determine relationships between pulsar parameters and the amplitude and timescale of timing noise. We show that the timing noise characteristics are consistent with young pulsars being dominated by the recovery from glitches, whereas the older pulsars are affected by pseudo-sinusoidal structures that could be due to free-precession of the neutron star.

Key words:

1 INTRODUCTION

The Jodrell Bank data archive of pulsar observations contains over 6000 years of pulsar rotational history. The basic observational parameters for the pulsars with data spanning more than six years were provided in Hobbs et al. (2004); hereafter Paper I. These timing ephemerides included the pulsar positions, rotational frequencies and their first two derivatives, dispersion measures and their derivatives and proper motions. The proper motions were updated with more recent observations and analysed in Hobbs et al. (2005). In this paper, we describe and quantify the structures observed in the timing residuals.

Structures previously observed in the timing residuals have been explained by unmodelled planetary companions (e.g. Cordes 1993), free-precession (e.g. Stairs, Lyne & Shemar 2000 who reported on free-precession in PSR B1828−11), glitches (Lyne, Shemar & Graham-Smith 2000) or timing noise (e.g. Lyne 1999). Glitches are thought to represent sudden increases in the pulsar's rotation rate. Timing noise describes a continuous, noise-like fluctuation in rotation rate.

The relationship between glitches and timing noise is not understood. Glitches are discrete events which occur more commonly in young pulsars (although for two pulsars with similar rotational parameters, one may glitch frequently while the other has never been observed to glitch) and seem to be divided into two sizes: most are large with fractional frequency increases of $\sim 10^{-6}$ while the smaller events are in the range 10^{-7} to 10^{-9}. No model currently predicts the time between glitches or the size of the event although pulsars with large glitches tend to show larger intervals between glitches (Lyne et al. 2000).

Much of the basic theoretical work carried out on timing noise was described in Boynton et al. (1972) who analysed the arrival times for the Crab pulsar over a two-year period. In this paper, an attempt was made to describe the timing noise as either phase (ϕ), frequency (ν) or slowing-down ($\dot{\nu}$) noise corresponding to random walks in these parameters. Later, Cordes & Helfand (1980) concluded that out of a sample of 11 pulsars, seven showed timing noise consistent with frequency noise, two from slowing-down noise and two from phase-noise. Cordes & Helfand (1980) concluded that 1) timing noise is widespread in pulsars, 2) it is correlated with period derivative and weakly with period, 3) is not correlated with height above the Galactic plane, luminosity nor pulse shape changes. However, Cordes & Downs (1985) showed that the idealized, large-rate random walk process was too simple. They developed a more detailed model where discrete 'micro-jumps' in one or more of the timing parameters are superimposed on the random walk process. D'Alessandro et al. (1995) analysed the timing residuals for 45 pulsars with data spanning up to seven years. 19 of their pulsars show very weak timing noise, for seven the activity is attributed to random walk processes comprising a large number of events in one of the rotation variables, a further seven are explained as resolved jumps in ν and $\dot{\nu}$ superimposed on a random walk process, seven more as resolved jumps on a low-level activity background and for the remaining five the timing noise cannot be due to a pure random walk process or resolved jumps.

The majority of analyses undertaken to understand pulsar timing noise have used relatively short data spans of <10 yr. However, a few recent papers have studied much longer data spans for a few pulsars. Scott, Finger & Wilson (2003) reported on the timing noise of the Crab pulsar over a 7 year interval, the study of PSR B1642−03 over a 30 year data span (Shabanova, Lyne & Urama 2001), a 16 year data span for PSR B0329+54 (Shabanova 1995), a 13 year data span for PSR B1828−11 (Stairs, Lyne & Shemar 2000), four pulsars for 14 years (Baykal et al. 1999), 12 years for PSR J1713+0747 (Splaver et al 2004) and 21 years of timing for PSR B1509−58 (Livingstone et al. 2005). **discuss the recent science paper and its implications for timing noise**

In this paper, we first show and describe the structures observed in the timing residuals for 370 pulsars with the shortest data span being 10 years and the longest over 35 years. This allows us to catagorize the forms seen in the timing residuals. We tabulate and analyse the amplitude and timescale of the timing noise and their relation with other pulsar parameters. We calculate and compare various stability parameters used to provide a measure of the amount of timing noise in any particular pulsar data set. We conclude the paper with a periodogram analysis of the timing residuals which allows us to study the spectrum of timing noise and to search for periodicities in the data.

An understanding of pulsar timing noise will lead to many important results. For instance, pulsar timing array projects are being developed around the world with the aim of detecting gravitational waves by looking for irregularities in the timing of millisecond pulsars (Hobbs 2005 and references therein). The gravitational wave signature from a stochastic background of coalescing binary black hole systems is expected to produce signatures in the timing residuals with amplitudes of approximately 100 ns. If the intrinsic timing noise for millisecond pulsars are at a higher level, then it will become extremely difficult to extract the gravitational wave signal from the observations. Explaining the cause of timing noise and glitches in the young pulsars may allow us to relate these phenomena and provide an insight into the interior structure of a neutron star.

2 RESULTS

The timing solutions for the pulsars in our sample have been updated using recent data available from the Jodrell Bank Observatory data archive. The timing solutions were obtained in an identical manner to that described in Paper I. In brief, the majority of the observations were obtained from the 76-m Lovell radio telescope at Jodrell Bank Observatory. The earliest times-of-arrival (TOAs) for 18 pulsars were obtained from observations using the NASA Deep Space Network (Downs & Reichley 1983). Observations using the Lovell telescope were carried at predominately at frequencies close to 408, 610, 910, 1410 and 1630 MHz with a few early observations at 235 and 325 MHz. The signals were combined to produce, for every observation, a total intensity profile. TOAs were subsequently determined by convolving, in the time domain, the profile with a template corresponding to the observing frequency. The pulsar timing residuals were obtained by fitting a timing model to the TOAs using the TEMPO2 pulsar timing software (Hobbs, Edwards, Manchester 2006).

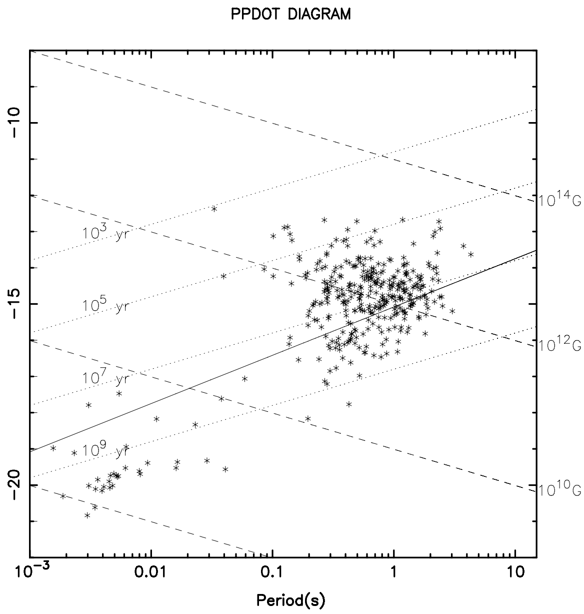

Figure 2. P–$\dot{\mathrm{P}}$ diagram for the pulsars in our sample.

In Figure 1 we plot the timing residuals for all the pulsars in our sample. The horizontal scale of each panel represents 35 years of observations and the vertical is scaled for each seperate panel. The upper value gives the range from the minimum to the maximum residual in milliseconds. The lower values give the same range, but in units of the pulsars' rotational periods.

In Table 1 we present the basic parameters for these pulsars. In column order, we first provide the pulsar's J2000 and B1950 names, spin-frequency, ν, frequency derivative, $\dot{\nu}$, and frequency second derivative, $\ddot{\nu}$. The next two columns give the logarithm of the pulsar's characteristic age, $\tau_c = -\nu/(2\dot{\nu})$ in years and the surface magnetic flux density $B_s = 3.2 \times 10^{19}\sqrt{\dot{\nu}/\nu^3}$. The following three columns gives the epoch of the centre of the data span, the number of observations and the time span of the observations. The final columns give σ_1 the unweighted rms of the residuals after fitting for a quadratic term, σ_2 the unweighted rms of the residuals after removal of a cubic term and σ_3 the whitened rms residuals. For the recycled pulsars[1] the unweighted rms of the residuals after subtracting a cubic term range from $\sim$10μs for PSRs J1713+0747 and J1744−1134 to 850μs for the globular cluster pulsar PSR B1820−30A and 430μs for PSR B1953+29. For the ordinary pulsars the rms ranges to 948 ms for PSR B1706−16 which is a pulsar with a 653 ms spin-period. A period–period derivative diagram for the pulsars in our sample is shown in Figure 2.

[1] Our sample includes 31 recycled pulsars defined as pulsars with spin-periods, $P < 0.1$ s and spin-down rates, $\dot{P} < 10^{-17}$.

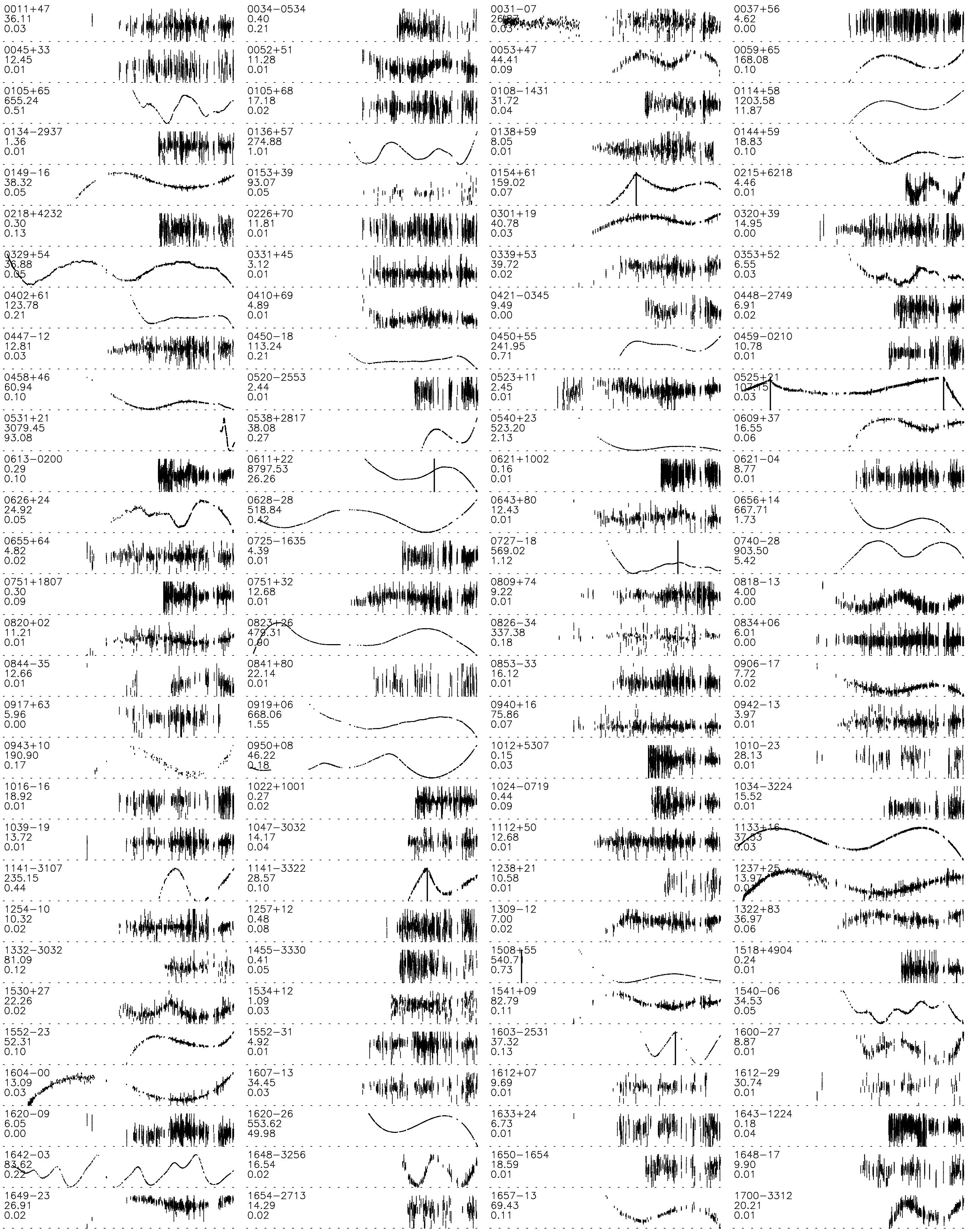

Figure 1. Timing residuals after subtraction of the pulsar's spin frequency and its first derivative. Vertical lines indicate epochs at which glitch events have been reported. The three labels on the left provide the pulsar name, the range from the minimum to maximum residual (ms) and the same range scaled with the pulsar's rotational period.

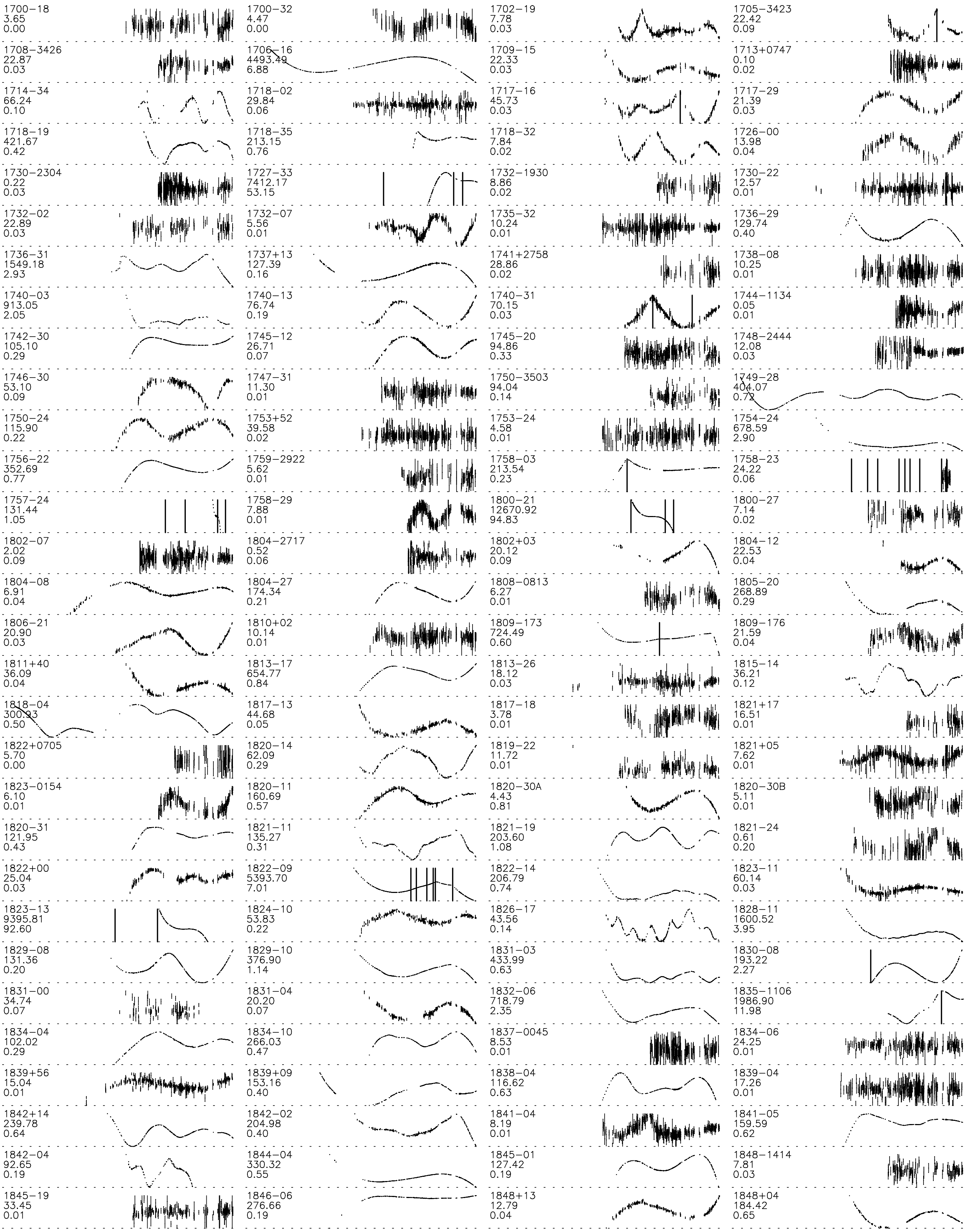

Figure 1. . . . continued

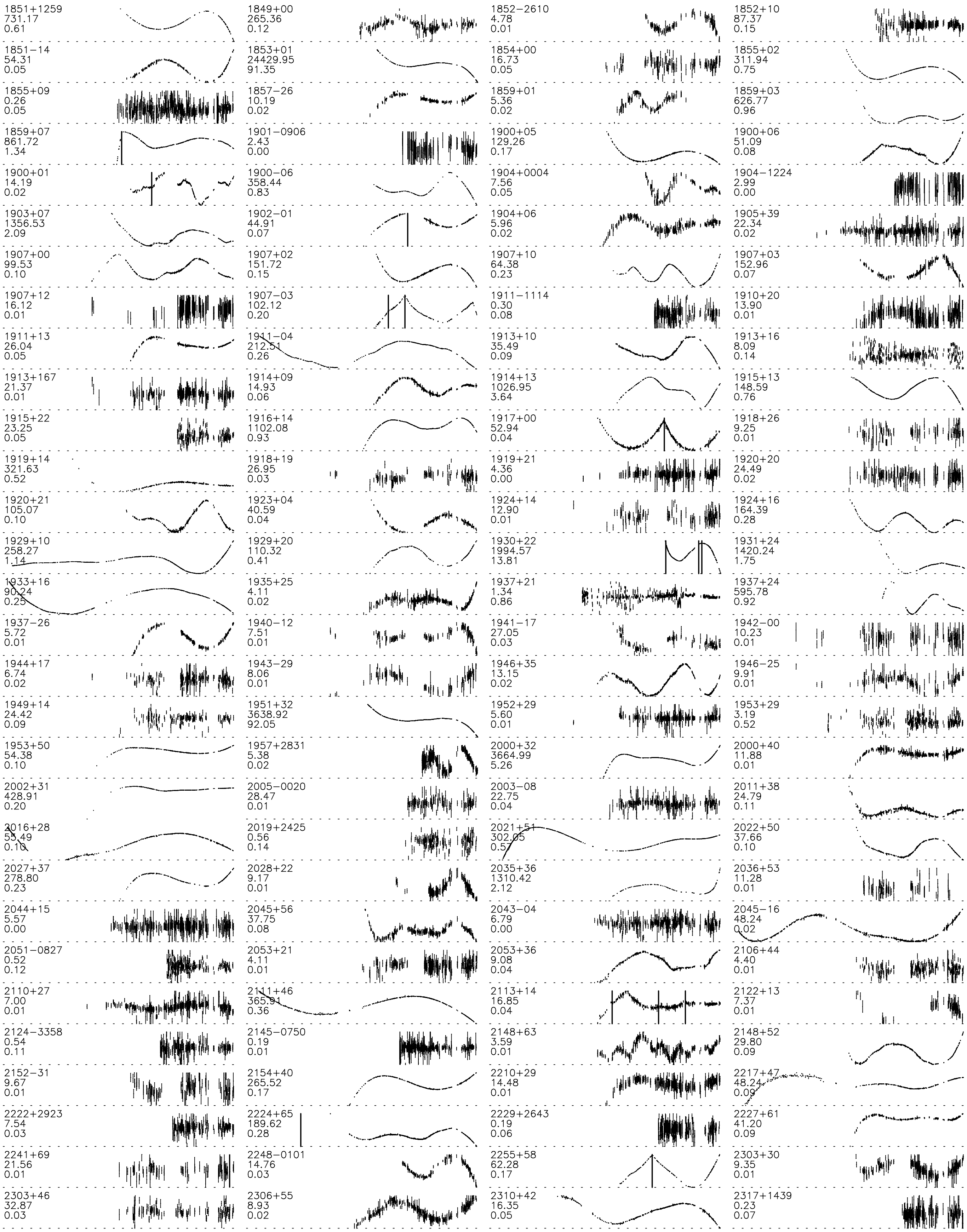

Figure 1. . . . continued

Table 1. Basic parameters for the pulsars in our sample. σ_1 is the rms residual after removing a quadratic term, σ_2, the rms value after removing a cubic term and σ_3 the value after whitening the data.

PSR J	PSR B	ν (s^{-1})	$\dot{\nu}$ ($10^{-15} s^{-2}$)	$\ddot{\nu}$ ($10^{-24} s^{-3}$)	$\log_{10}(\tau_c)$	$\log_{10}$ B_s (G)	Epoch (MJD)	N	T_{span} (yr)	σ_1 (ms)	σ_2 (ms)	σ_3 (ms)
J0014+4746	B0011+47	0.806	−0.367	+0.00035(20)	7.54	11.93	49285.0	365	22.8	4.25	4.23	4.19
J0034−0534	—	532.713	−1.409	−0.045(10)	9.78	7.99	51096.0	402	12.8	0.06	0.06	0.05
J0034−0721	B0031−07	1.061	−0.459	+0.00033(3)	7.56	11.80	47051.0	772	35.0	3.77	3.47	3.37
J0040+5716	B0037+56	0.894	−2.302	−0.00005(6)	6.79	12.26	50091.0	425	18.5	0.62	0.62	0.61
J0048+3412	B0045+33	0.822	−1.589	−0.0003(3)	6.91	12.23	50083.0	200	18.4	2.18	2.16	2.11
J0055+5117	B0052+51	0.473	−2.132	+0.00092(5)	6.55	12.66	50092.0	416	18.5	1.48	1.08	1.00
J0056+4756	B0053+47	2.118	−14.938	−0.0083(18)	6.35	12.10	50103.0	251	17.2	5.78	5.73	2.28
J0102+6537	B0059+65	0.596	−2.113	−0.02862(17)	6.65	12.51	50091.0	338	18.5	24.49	2.53	1.29
J0108+6608	B0105+65	0.779	−7.918	+0.107(16)	6.19	12.62	50482.0	426	16.1	156.51	148.47	12.21
J0108+6905	B0105+68	0.934	−0.042	−0.0002(3)	8.55	11.36	50091.0	335	18.5	2.63	2.62	2.59
J0108−1431	—	1.238	−0.118	−0.0030(18)	8.22	11.40	51251.0	332	12.1	4.49	4.47	4.38
J0117+5914	B0114+58	9.858	−568.596	−2.91(3)	5.44	11.89	50083.0	313	18.2	160.88	25.74	0.70
J0134−2937	—	7.301	−4.178	−0.0004(5)	7.44	11.02	51251.0	298	12.1	0.19	0.19	0.18
J0139+5814	B0136+57	3.670	−144.309	−0.065(10)	5.61	12.24	49706.0	683	20.6	54.30	52.30	2.05
J0141+6009	B0138+59	0.818	−0.261	+0.00029(6)	7.70	11.84	49495.0	450	19.4	1.09	1.06	1.04
J0147+5922	B0144+59	5.094	−6.661	+0.0255(7)	7.08	11.36	50080.0	429	17.3	2.60	1.16	0.17
J0152−1637	B0149−16	1.201	−1.874	−0.00425(5)	7.01	12.02	48651.0	454	25.5	5.63	1.39	0.59
J0156+3949	B0153+39	0.552	−0.046	−0.0001(12)	8.27	11.73	50104.0	80	16.5	10.00	10.00	9.00
J0157+6212	B0154+61	0.425	−34.159	−0.0093(8)	5.29	13.33	50126.0	462	18.1	22.84	20.14	2.43
J0215+6218	—	1.822	−2.198	−0.0022(12)	7.12	11.79	51788.0	294	9.4	0.92	0.92	0.43
J0218+4232	—	430.461	−14.340	−0.007(8)	8.68	8.63	51268.0	387	11.9	0.05	0.05	0.05
J0231+7026	B0226+70	0.682	−1.445	+0.00026(13)	6.87	12.33	50088.0	304	18.5	1.83	1.82	1.75
J0304+1932	B0301+19	0.721	−0.673	−0.00274(7)	7.23	12.13	49141.0	498	23.7	3.90	1.76	0.95
J0323+3944	B0320+39	0.330	−0.069	+0.00004(4)	7.88	12.15	49229.0	519	23.2	2.25	2.24	2.20
J0332+5434	B0329+54	1.400	−4.012	+0.00092(7)	6.74	12.09	46775.0	1169	36.5	7.38	6.76	0.50
J0335+4555	B0331+45	3.715	−0.101	+0.00014(12)	8.76	10.65	50081.0	482	18.2	0.33	0.33	0.32
J0343+5312	B0339+53	0.517	−3.587	−0.00131(15)	6.36	12.71	49557.0	325	22.9	4.64	4.14	3.97
J0357+5236	B0353+52	5.075	−12.277	+0.0078(4)	6.82	11.49	50081.0	411	18.2	0.95	0.63	0.21
J0406+6138	B0402+61	1.682	−15.773	+0.0476(19)	6.23	12.27	50428.0	406	16.7	13.75	8.44	0.57
J0415+6954	B0410+69	2.559	−0.502	+0.00142(11)	7.91	11.24	50092.0	374	18.5	0.47	0.40	0.36
J0421−0345	—	0.463	−0.249	+0.0019(5)	7.47	12.21	50847.0	140	9.7	1.28	1.21	1.17
J0448−2749	—	2.220	−0.731	−0.0029(9)	7.68	11.42	51427.0	331	11.2	0.88	0.86	0.85
J0450−1248	B0447−12	2.283	−0.535	−0.0010(3)	7.83	11.33	49751.0	526	19.7	1.68	1.65	1.63
J0452−1759	B0450−18	1.822	−19.092	+0.0137(5)	6.18	12.25	49295.0	576	22.9	8.20	5.15	0.30
J0454+5543	B0450+55	2.935	−20.441	−0.184(4)	6.36	11.96	50336.0	334	17.2	27.68	10.00	0.38
J0459−0210	—	0.883	−1.089	−0.0004(5)	7.11	12.11	51269.0	238	12.0	1.34	1.34	1.32
J0502+4654	B0458+46	1.566	−13.690	+0.01057(16)	6.26	12.28	49129.0	497	23.6	7.24	2.20	0.55
J0520−2553	—	4.138	−0.515	+0.0026(12)	8.10	10.94	51657.0	181	10.2	0.42	0.41	0.40
J0525+1115	B0523+11	2.821	−0.586	−0.000239(20)	7.88	11.21	48663.0	642	26.3	0.32	0.28	0.27
J0528+2200	B0525+21	0.267	−2.854	+0.00082(4)	6.17	13.09	46909.0	954	35.8	20.18	15.26	1.44
J0538+2817	—	6.985	−179.088	−0.6718(18)	5.79	11.87	51821.0	313	9.0	6.55	0.29	0.18
J0543+2329	B0540+23	4.065	−254.893	+0.1707(20)	5.40	12.29	49294.0	691	22.9	37.82	14.53	0.19
J0612+3721	B0609+37	3.356	−0.670	−0.0125(3)	7.90	11.13	50092.0	455	18.5	2.00	0.80	0.36
J0613−0200	—	326.601	−1.019	+0.009(4)	9.71	8.24	51240.0	655	12.1	0.04	0.04	0.04
J0614+2229	B0611+22	2.985	−529.523	+8.35(8)	4.95	12.65	50164.0	970	18.1	1502.68	404.91	40.85
J0621+1002	—	34.657	−0.057	+0.0011(5)	9.99	9.07	51145.0	634	9.6	0.02	0.02	0.02
J0624−0424	B0621−04	0.962	−0.769	+0.00001(10)	7.30	11.97	50302.0	458	17.3	0.87	0.87	0.84
J0629+2415	B0626+24	2.098	−8.785	+0.0049(8)	6.58	11.99	49846.0	541	19.7	5.75	5.53	0.58
J0630−2834	B0628−28	0.804	−4.601	−0.0175(7)	6.44	12.48	47013.0	806	35.1	131.71	91.58	1.54
J0653+8051	B0643+80	0.823	−2.576	+0.00069(4)	6.70	12.34	49141.0	283	23.7	1.23	0.83	0.71
J0659+1414	B0656+14	2.598	−371.288	+0.7636(19)	5.04	12.67	49721.0	771	16.1	106.66	7.22	1.59
J0700+6418	B0655+64	5.111	−0.018	+0.00019(13)	9.66	10.07	49138.0	402	23.7	0.64	0.64	0.60
J0725−1635	—	2.357	−0.515	+0.0015(10)	7.86	11.30	50884.0	176	9.9	0.60	0.60	0.57
J0729−1836	B0727−18	1.960	−72.832	+0.245(7)	5.63	12.50	50126.0	634	18.3	73.73	39.66	3.42
J0742−2822	B0740−28	5.997	−604.876	−0.61(5)	5.20	12.23	49696.0	1009	20.6	160.98	140.42	5.35
J0751+1807	—	287.458	−0.643	−0.002(4)	9.85	8.22	51389.0	530	11.3	0.04	0.04	0.04
J0754+3231	B0751+32	0.693	−0.519	−0.00081(6)	7.33	12.10	49763.0	491	19.8	1.54	1.28	1.22
J0814+7429	B0809+74	0.774	−0.101	+0.00014(5)	8.09	11.67	49369.0	473	22.1	1.07	1.06	1.03
J0820−1350	B0818−13	0.808	−1.373	+0.000028(19)	6.97	12.21	49299.0	631	22.7	0.55	0.55	0.27
J0823+0159	B0820+02	1.156	−0.140	−0.00074(5)	8.12	11.48	49144.0	573	23.7	1.10	0.88	0.84
J0826+2637	B0823+26	1.884	−6.069	+0.0240(12)	6.69	11.98	46857.0	978	36.1	110.69	90.20	0.50
J0828−3417	B0826−34	0.541	−0.292	−0.0035(4)	7.47	12.14	48508.0	145	25.9	19.28	15.84	12.98
J0837+0610	B0834+06	0.785	−4.191	+0.000102(11)	6.47	12.47	49138.0	536	23.7	0.36	0.34	0.32
J0846−3533	B0844−35	0.896	−1.285	+0.00107(13)	7.04	12.13	49145.0	119	23.7	1.96	1.53	1.41
J0849+8028	B0841+80	0.624	−0.174	+0.00005(74)	7.76	11.93	50419.0	90	16.6	4.82	4.82	4.44
J0855−3331	B0853−33	0.789	−3.934	+0.00059(15)	6.50	12.46	49735.5	434	17.2	1.63	1.60	1.57
J0908−1739	B0906−17	2.490	−4.151	+0.00165(5)	6.98	11.72	49140.0	639	23.7	0.73	0.43	0.29
J0921+6254	B0917+63	0.638	−1.468	+0.00018(12)	6.84	12.38	49687.0	156	16.3	0.86	0.85	0.78
J0922+0638	B0919+06	2.322	−73.982	+0.1385(12)	5.70	12.39	48518.0	765	27.0	97.96	22.19	2.53
J0943+1631	B0940+16	0.920	−0.077	+0.00008(16)	8.28	11.50	49143.0	443	23.7	4.05	4.04	3.96
J0944−1354	B0942−13	1.754	−0.139	−0.00027(5)	8.30	11.21	49764.0	532	19.8	0.41	0.40	0.39
J0946+0951	B0943+10	0.911	−2.902	−0.0377(8)	6.70	12.30	49352.0	117	22.3	47.99	10.33	9.51
J0953+0755	B0950+08	3.952	−3.588	−0.0048(3)	7.24	11.39	46777.0	953	36.5	11.19	9.54	0.40
J1012+5307	—	190.268	−0.620	+0.0030(12)	9.69	8.48	51331.0	521	11.6	0.02	0.02	0.02
J1012−2337	B1010−23	0.397	−0.139	+0.00012(12)	7.66	12.18	49127.0	137	23.6	4.59	4.57	4.26
J1018−1642	B1016−16	0.554	−0.535	+0.00006(18)	7.22	12.25	50093.0	243	18.5	2.79	2.79	2.70
J1022+1001	—	60.779	−0.160	−0.0004(8)	9.78	8.93	51638.0	630	9.9	0.03	0.03	0.03
J1024−0719	—	193.716	−0.695	+0.007(6)	9.64	8.50	51422.0	365	10.9	0.06	0.06	0.06
J1034−3224	—	0.869	−0.174	−0.0005(6)	7.90	11.72	51123.0	224	12.9	1.83	1.83	1.75
J1041−1942	B1039−19	0.721	−0.492	−0.0000009(500)	7.37	12.06	49143.0	477	23.7	1.31	1.31	1.29
J1047−3032	—	3.027	−0.559	−0.004(3)	7.93	11.16	51445.0	263	11.1	1.85	1.84	1.82
J1115+5030	B1112+50	0.604	−0.909	−0.00006(5)	7.02	12.31	49753.0	490	19.7	1.29	1.28	1.26
J1136+1551	B1133+16	0.842	−2.646	+0.00047(5)	6.70	12.33	46407.0	900	36.4	9.11	8.66	0.25
J1141−3107	—	1.857	−6.880	−0.61(3)	6.63	12.02	51271.0	178	12.0	70.21	37.88	3.11
J1141−3322	—	6.862	−10.921	−0.291(14)	7.00	11.27	51446.0	327	11.1	6.56	4.23	0.63
J 1238+21	B1238+21	0.894	−1.155	−0.003(3)	7.09	12.11	51822.0	72	8.9	1.86	1.85	1.77
J1239+2453	B1237+25	0.723	−0.502	−0.000350(7)	7.36	12.07	46942.0	1026	35.6	2.70	1.41	0.59
J1257−1027	B1254−10	1.620	−0.952	−0.00009(16)	7.43	11.68	49348.2	475	18.4	1.12	1.12	1.08
J1300+1240	B1257+12	160.810	−2.957	+0.002(4)	8.94	8.93	50788.0	360	14.5	0.08	0.08	0.08
J1311−1228	B1309−12	2.235	−0.753	−0.00141(12)	7.67	11.42	50094.0	433	18.5	0.65	0.56	0.50

PSR J	PSR B	ν (s^{-1})	$\dot{\nu}$ ($10^{-15} s^{-2}$)	$\ddot{\nu}$ ($10^{-24} s^{-3}$)	$\log_{10}(\tau_c)$	$\log_{10} B_s$ (G)	Epoch (MJD)	N	T_{span} (yr)	σ_1 (ms)	σ_2 (ms)	σ_3 (ms)
J1321+8323	B1322+83	1.492	−1.262	−0.0056(3)	7.27	11.79	49282.0	289	22.8	3.97	2.31	2.17
J1332−3032	—	1.537	−1.322	+0.017(9)	7.27	11.79	51447.0	191	11.0	9.66	9.57	9.04
J1455−3330	—	125.200	−0.381	−0.008(4)	9.72	8.65	51190.0	269	12.4	0.07	0.07	0.07
J1509+5531	B1508+55	1.352	−9.144	+0.0819(15)	6.37	12.29	49294.0	470	22.7	59.55	22.06	0.55
J1518+4904	—	24.429	−0.016	+0.0002(5)	10.38	9.03	51619.0	308	9.9	0.03	0.03	0.03
J1532+2745	B1530+27	0.889	−0.616	−0.0024(3)	7.36	11.98	50096.0	414	18.5	3.37	3.04	1.66
J1537+1155	B1534+12	26.382	−1.686	+0.00004(26)	8.39	9.99	50300.0	399	13.8	0.04	0.04	0.04
J1543+0929	B1541+09	1.336	−0.772	−0.0093(4)	7.44	11.76	49141.0	451	23.7	10.40	6.46	3.27
J1543−0620	B1540−06	1.410	−1.749	+0.0130(3)	7.11	11.90	49839.0	502	19.7	6.98	3.03	0.44
J1555−2341	B1552−23	1.878	−2.447	−0.0280(4)	7.08	11.79	50301.0	346	17.3	6.42	1.40	0.89
J1555−3134	B1552−31	1.930	−0.232	−0.00018(19)	8.12	11.26	50299.0	289	17.3	0.70	0.69	0.67
J1603−2531	—	3.533	−19.875	−0.068(12)	6.45	11.83	51121.0	191	12.0	9.09	8.19	0.43
J1603−2712	B1600−27	1.285	−4.968	−0.0025(3)	6.61	12.19	50302.0	199	17.3	1.61	1.37	0.67
J1607−0032	B1604−00	2.371	−1.720	−0.002015(10)	7.34	11.56	47386.0	728	33.2	3.54	0.47	0.44
J1610−1322	B1607−13	0.982	−0.222	−0.0003(6)	7.85	11.69	50094.0	213	18.5	4.76	4.76	4.65
J1614+0737	B1612+07	0.829	−1.620	−0.0007(3)	6.91	12.23	49897.0	160	15.1	1.15	1.12	1.07
J1615−2940	B1612−29	0.404	−0.258	+0.00012(17)	7.39	12.30	49026.0	98	23.1	4.88	4.87	4.62
J1623−0908	B1620−09	0.783	−1.584	+0.00027(3)	6.89	12.26	49142.0	393	23.7	0.84	0.76	0.71
J1623−2631	B1620−26	90.287	−2.953	+18.346(11)	8.69	9.31	50292.0	767	17.5	103.67	3.06	0.15
J1635+2418	B1633+24	2.039	−0.496	+0.00070(20)	7.81	11.39	49130.0	148	16.6	1.19	1.19	1.16
J1643−1224	—	216.373	−0.865	−0.0044(19)	9.60	8.47	51251.0	432	12.0	0.03	0.03	0.02
J1645−0317	B1642−03	2.579	−11.846	+0.0053(5)	6.54	11.92	46930.0	956	35.6	21.70	20.05	1.21
J1648−3256	—	1.390	−6.815	+0.004(3)	6.51	12.21	51276.0	148	12.0	4.54	4.51	0.83
J1650−1654	—	0.572	−1.046	−0.0027(8)	6.94	12.38	51272.0	171	12.0	3.06	2.93	2.77
J1651−1709	B1648−17	1.027	−3.205	+0.0007(4)	6.71	12.24	50430.0	167	16.3	1.56	1.54	1.36
J1652−2404	B1649−23	0.587	−1.088	−0.00155(5)	6.93	12.37	49132.0	347	23.6	3.17	1.70	1.60
J1654−2713	—	1.263	−0.268	+0.002(3)	7.87	11.57	51414.0	154	11.1	2.40	2.39	2.36
J1659−1305	B1657−13	1.560	−1.503	+0.0309(7)	7.22	11.80	50094.0	145	18.5	10.87	2.68	2.37
J1700−3312	—	0.736	−2.555	−0.0163(6)	6.66	12.41	51276.0	249	12.0	3.93	1.88	1.46
J1703−1846	B1700−18	1.243	−2.676	+0.00003(12)	6.87	12.08	50314.0	209	17.3	0.56	0.56	0.52
J1703−3241	B1700−32	0.825	−0.449	+0.00122(9)	7.46	11.96	50427.0	158	16.3	0.77	0.51	0.48
J1705−1906	B1702−19	3.345	−46.284	−0.0009(6)	6.06	12.05	50497.0	410	16.3	1.25	1.24	0.36
J1705−3423	—	3.915	−16.484	+0.085(6)	6.58	11.72	51256.0	151	11.9	4.63	2.86	1.11
J1708−3426	—	1.445	−8.775	−0.0101(14)	6.42	12.24	51276.0	123	12.0	2.43	2.07	1.98
J1709−1640	B1706−16	1.531	−14.780	+0.3397(11)	6.22	12.31	47389.0	484	33.2	837.06	156.71	0.93
J1711−1509	B1709−15	1.151	−1.461	+0.0067(3)	7.10	12.00	50094.0	197	18.5	3.77	1.72	0.68
J1713+0747	—	218.812	−0.409	+0.0020(13)	9.93	8.30	51318.0	344	11.5	0.01	0.01	0.01
J1717−3425	B1714−34	1.524	−22.761	+0.022(8)	6.03	12.41	50673.0	138	15.2	17.92	17.45	1.38
J1720−0212	B1718−02	2.093	−0.363	−0.0001(6)	7.96	11.30	49853.0	319	19.8	3.45	3.45	3.39
J1720−1633	B1717−16	0.639	−2.366	−0.00002(72)	6.63	12.48	50084.0	207	18.4	9.09	9.09	1.43
J1720−2933	B1717−29	1.612	−1.938	−0.0142(3)	7.12	11.84	50290.0	164	17.2	3.89	0.87	0.70
J1721−1936	B1718−19	0.996	−1.609	+0.153(13)	6.99	12.11	50840.0	288	14.4	67.67	54.78	5.31
J1721−3532	B1718−35	3.566	−320.260	−0.07(6)	5.25	12.43	51505.0	138	10.2	14.95	15.94	3.33
J1722−3207	B1718−32	2.096	−2.838	−0.0010(7)	7.07	11.75	50495.0	180	16.3	1.72	1.71	0.22
J1728−0007	B1726−00	2.591	−7.535	−0.0167(7)	6.74	11.82	50513.0	151	16.1	2.89	1.29	0.95
J1730−2304	—	123.110	−0.306	−0.0060(13)	9.80	8.61	51240.0	443	12.0	0.03	0.03	0.03
J1730−3350	B1727−33	7.170	−4361.164	−51.5(20)	4.42	12.54	51419.0	351	11.2	1204.52	491.30	197.19
J1732−1930	—	2.067	−0.776	−0.004(3)	7.63	11.48	51644.0	99	10.1	1.41	1.40	1.36
J1733−2228	B1730−22	1.147	−0.056	−0.00006(8)	8.51	11.29	49140.0	394	23.7	1.41	1.40	1.39
J1734−0212	B1732−02	1.191	−0.597	+0.0026(8)	7.50	11.78	50117.0	127	18.3	3.52	3.37	3.22
J1735−0724	B1732−07	2.385	−6.908	+0.0019(4)	6.74	11.86	50312.0	342	17.3	1.22	1.18	0.26
J1738−3211	B1735−32	1.301	−1.346	+0.00043(14)	7.19	11.90	50018.0	360	18.9	1.33	1.31	1.28
J1739−2903	B1736−29	3.097	−75.578	+0.127(4)	5.81	12.21	49872.0	392	18.9	28.56	10.50	1.45
J1739−3131	B1736−31	1.889	−66.269	+0.78(4)	5.65	12.50	49884.0	243	18.1	279.24	175.12	6.54
J1740+1311	B1737+13	1.245	−2.250	+0.01946(14)	6.94	12.04	48669.0	442	26.3	24.90	3.58	0.57
J1741+2758	—	0.735	−0.994	+0.001(6)	7.07	12.20	51750.0	71	9.4	4.72	4.72	4.64
J1741−0840	B1738−08	0.489	−0.545	−0.00007(10)	7.15	12.34	50306.0	295	17.2	1.34	1.34	1.33
J1743−0339	B1740−03	2.249	−7.873	+0.41(4)	6.66	11.93	50199.0	135	16.6	109.68	77.53	8.37
J1743−1351	B1740−13	2.467	−2.910	−0.080(3)	7.13	11.65	50095.0	184	18.5	19.33	8.55	1.14
J1743−3150	B1740−31	0.414	−20.716	−0.0184(7)	5.50	13.24	50674.0	280	15.3	16.67	8.66	2.74
J1744−1134	—	245.426	−0.539	−0.0075(12)	9.86	8.29	51490.0	281	10.7	0.01	0.01	0.01
J1745−3040	B1742−30	2.722	−79.021	−0.0629(18)	5.74	12.30	50311.0	393	17.3	10.44	4.97	0.19
J1748−1300	B1745−12	2.537	−7.808	−0.0347(7)	6.71	11.84	50315.0	289	17.3	5.89	1.86	0.28
J1748−2021	B1745−20	3.465	−4.803	+0.059(8)	7.06	11.54	50677.0	362	15.3	14.86	13.69	13.31
J1748−2444	—	2.258	−0.568	−0.0024(12)	7.80	11.35	50917.0	189	14.2	1.82	1.80	1.77
J1749−3002	B1746−30	1.640	−21.163	−0.0525(20)	6.09	12.35	50653.0	192	15.2	11.50	5.34	2.04
J1750−3157	B1747−31	1.098	−0.237	+0.0003(4)	7.87	11.63	50674.0	212	15.3	1.33	1.33	1.27
J1750−3503	—	1.462	−0.079	+0.031(16)	8.47	11.21	51426.0	131	11.2	15.94	15.71	14.94
J1752−2806	B1749−28	1.778	−25.687	+0.0087(10)	6.04	12.34	46889.0	654	35.8	66.82	63.08	1.11
J1753−2501	B1750−24	1.893	−50.565	−0.014(5)	5.77	12.44	49883.0	215	18.9	21.48	21.33	3.95
J1754+5201	B1753+52	0.418	−0.274	−0.0003(3)	7.38	12.29	50095.0	289	18.5	5.01	5.00	4.87
J1756−2435	B1753−24	1.491	−0.633	−0.00005(12)	7.57	11.65	49848.0	231	18.8	0.75	0.75	0.70
J1757−2421	B1754−24	4.272	−235.739	+0.140(4)	5.46	12.25	49121.0	396	22.8	37.47	17.55	1.54
J1759−2205	B1756−22	2.169	−51.171	−0.213(3)	5.83	12.36	50126.0	388	18.3	49.84	11.51	0.54
J1759−2922	—	1.741	−14.028	+0.0017(9)	6.29	12.22	51256.0	132	11.9	0.96	0.95	0.84
J1801−0357	B1758−03	1.085	−3.897	−0.032(3)	6.64	12.25	50084.0	201	18.4	22.60	16.77	1.20
J1801−2920	B1758−29	0.924	−2.814	−0.0041(8)	6.72	12.28	51417.0	228	11.0	1.58	1.50	0.61
J1803−2137	B1800−21	7.484	−7511.505	+220.36(3)	4.20	12.63	49527.0	356	6.9	954.70	47.85	3.18
J1803−2712	B1800−27	2.990	−0.153	+0.0012(7)	8.49	10.88	50661.0	151	15.1	1.17	1.18	1.10
J1804−0735	B1802−07	43.288	−0.875	+0.0036(14)	8.89	9.52	50709.0	432	15.0	0.28	0.28	0.28
J1804−2717	—	107.032	−0.468	−0.010(3)	9.56	8.80	51440.0	260	10.9	0.07	0.07	0.07
J1805+0306	B1802+03	4.572	−20.892	+0.04414(19)	6.54	11.67	50331.0	196	16.5	3.81	1.74	0.26
J1806−1154	B1804−12	1.913	−5.157	+0.0299(6)	6.77	11.94	51096.0	179	12.7	2.68	1.07	0.77
J1807−0847	B1804−08	6.108	−1.074	−0.003045(9)	7.95	10.84	48671.0	456	26.3	1.04	0.55	0.09
J1807−2715	B1804−27	1.208	−17.768	−0.08609(14)	6.03	12.51	50291.0	233	17.2	27.46	3.32	0.79
J1808−0813	—	1.141	−1.616	+0.0028(4)	7.05	12.02	51271.0	153	12.0	0.99	0.91	0.84
J1808−2057	B1805−20	1.089	−20.243	+0.07844(13)	5.93	12.60	49937.0	187	18.8	44.89	4.63	1.59
J1809−2109	B1806−21	1.424	−7.747	−0.00934(7)	6.46	12.22	49995.0	226	18.8	4.88	3.12	0.36
J1812+0226	B1810+02	1.260	−5.711	+0.0007(3)	6.54	12.23	50336.0	244	17.1	1.32	1.28	1.17
J1812−1718	—	0.830	−13.128	+0.08279(7)	6.00	12.69	49887.0	233	18.9	80.84	48.68	3.29

PSR J	PSR B	ν (s^{-1})	$\dot{\nu}$ ($10^{-15} s^{-2}$)	$\ddot{\nu}$ ($10^{-24} s^{-3}$)	$\log_{10}(\tau_c)$	$\log_{10} B_s$ (G)	Epoch (MJD)	N	T_{span} (yr)	σ_1 (ms)	σ_2 (ms)	σ_3 (ms)
J1812−1733	—	1.858	−3.390	−0.0134(8)	6.94	11.87	50688.0	191	15.2	3.81	3.01	2.81
J1813+4013	B1811+40	1.074	−2.939	+0.01290(12)	6.76	12.19	50300.0	266	17.2	5.02	1.16	0.88
J1816−1729	B1813−17	1.278	−11.873	−0.20505(10)	6.23	12.38	49887.0	237	18.8	99.19	16.47	1.10
J1816−2650	B1813−26	1.687	−0.189	−0.00109(10)	8.15	11.30	49573.9	260	23.6	2.04	1.88	1.84
J1818−1422	B1815−14	3.431	−23.995	−0.01865(10)	6.36	11.89	49993.0	217	18.6	8.77	8.34	0.96
J1820−0427	B1818−04	1.672	−17.700	+0.0269096(15)	6.18	12.29	47020.0	690	35.1	91.86	46.26	0.75
J1820−1346	B1817−13	1.085	−5.294	+0.01260(12)	6.51	12.31	50018.0	217	18.9	7.77	2.01	1.26
J1820−1818	B1817−18	3.227	−0.975	+0.0039(5)	7.72	11.24	50663.0	170	15.1	0.71	0.58	0.55
J 1821+17	B1821+17	0.732	−0.466	+0.0003(19)	7.40	12.04	51819.0	91	9.0	2.52	2.53	2.52
J1822+0705	—	0.734	−0.941	+0.0011(13)	7.09	12.19	51748.0	78	9.4	1.12	1.13	1.12
J1822−1400	B1820−14	4.656	−19.665	−0.1110(3)	6.57	11.65	50042.0	207	18.6	16.75	9.97	1.00
J1822−2256	B1819−22	0.534	−0.385	+0.00013(10)	7.34	12.21	49120.0	164	16.0	1.11	1.11	1.07
J1823+0550	B1821+05	1.328	−0.400	−0.00149(5)	7.72	11.62	49844.0	354	19.4	1.01	0.58	0.36
J1823−0154	—	1.316	−1.960	−0.0088(4)	7.03	11.97	51276.0	155	12.0	1.35	0.71	0.57
J1823−1115	B1820−11	3.574	−17.611	−0.1563(5)	6.51	11.80	49993.0	448	18.6	25.98	11.65	2.98
J1823−3021	—	183.823	−114.337	+0.528(3)	7.41	9.64	50719.0	301	15.0	0.84	0.09	0.09
J1823−3021	—	2.641	−0.225	+0.0032(4)	8.27	11.05	50700.0	302	14.9	0.78	0.72	0.64
J1823−3106	B1820−31	3.520	−36.278	−0.12980(5)	6.19	11.97	50315.0	237	17.3	17.69	8.32	0.35
J1824−1118	B1821−11	2.295	−18.716	+0.05739(12)	6.29	12.10	49874.0	232	18.7	25.95	20.53	1.74
J1824−1945	B1821−19	5.282	−145.939	−0.17194(4)	5.76	12.00	50101.0	351	18.2	36.93	34.03	0.53
J1824−2452	B1821−24	327.406	−173.519	+0.049(5)	7.48	9.35	50238.0	162	17.4	0.13	0.11	0.09
J1825+0004	B1822+00	1.284	−1.445	−0.00788(14)	7.15	11.92	50336.0	238	17.1	3.30	2.22	0.63
J1825−0935	B1822−09	1.300	−88.369	+1.54726(3)	5.37	12.81	49831.0	503	19.7	759.34	173.46	16.36
J1825−1446	B1822−14	3.582	−290.948	+0.18805(10)	5.29	12.41	49862.0	233	19.1	33.63	8.70	1.51
J1826−1131	B1823−11	0.478	−1.121	+0.00419(7)	6.83	12.51	49867.0	339	19.7	6.76	3.20	2.41
J1826−1334	B1823−13	9.856	−7294.596	+147.730(5)	4.33	12.45	50639.9	237	7.8	705.55	30.29	6.48
J1827−0958	B1824−10	4.069	−16.597	−0.0398(4)	6.59	11.70	49883.0	252	18.8	6.86	3.64	1.80
J1829−1751	B1826−17	3.256	−58.853	+0.05928(5)	5.94	12.12	50101.0	363	18.2	10.50	7.69	1.82
J1830−1059	B1828−11	2.469	−365.841	+0.841539(17)	5.03	12.70	50031.0	754	18.7	187.26	18.07	10.32
J1832−0827	B1829−08	1.545	−152.462	−0.02462(4)	5.21	12.81	49868.0	358	18.8	28.04	27.42	0.61
J1832−1021	B1829−10	3.027	−38.493	+0.25131(9)	6.10	12.08	49883.0	371	18.8	50.10	9.82	0.70
J1833−0338	B1831−03	1.456	−88.139	+0.09744(4)	5.42	12.73	50123.0	499	18.3	44.27	31.26	2.87
J1833−0827	B1830−08	11.725	−1260.890	−1.3659(4)	5.17	11.95	50740.0	350	14.7	31.25	3.54	0.34
J1834−0010	B1831−00	1.920	−0.039	−0.0030(18)	8.89	10.88	49123.0	148	12.8	5.42	5.48	5.20
J1834−0426	B1831−04	3.447	−0.854	+0.02158(18)	7.81	11.16	50165.0	250	18.1	3.21	1.25	0.49
J1835−0643	B1832−06	3.270	−432.507	+0.7941(5)	5.08	12.55	49993.0	254	18.8	148.66	27.75	2.17
J1835−1106	—	6.027	−748.767	+9.0989(4)	5.11	12.27	51289.0	242	12.1	319.72	180.82	43.26
J1836−0436	B1834−04	2.823	−13.239	−0.06576(8)	6.53	11.89	49957.0	246	19.2	16.92	7.55	0.51
J1836−1008	B1834−10	1.777	−37.278	−0.01277(4)	5.88	12.42	50123.0	278	17.3	35.35	35.99	1.31
J1837−0045	—	1.621	−4.424	−0.0031(16)	6.76	12.01	51400.0	193	11.0	1.40	1.38	1.38
J1837−0653	B1834−06	0.525	−0.213	−0.00003(13)	7.59	12.09	50014.0	240	18.5	3.11	3.11	3.02
J1840+5640	B1839+56	0.605	−0.547	−0.000906(16)	7.24	12.20	49129.0	368	23.6	2.01	1.09	1.05
J1841+0912	B1839+09	2.622	−7.496	+0.045286(19)	6.74	11.81	48854.0	374	25.3	28.07	13.47	1.17
J1841−0425	B1838−04	5.372	−184.441	+0.04131(7)	5.66	12.04	49849.0	319	18.6	21.77	22.29	0.39
J1842−0359	B1839−04	0.543	−0.150	+0.00038(10)	7.76	11.99	49848.0	302	19.6	2.73	2.69	2.63
J1844+1454	B1842+14	2.663	−13.281	+0.04488(4)	6.50	11.93	49766.0	386	20.3	42.19	40.60	0.90
J1844−0244	B1842−02	1.970	−64.936	+0.0765(3)	5.68	12.47	49884.0	243	19.2	35.87	26.13	2.29
J1844−0433	B1841−04	1.009	−3.986	−0.00112(7)	6.60	12.30	50032.0	348	18.8	1.41	1.22	0.71
J1844−0538	B1841−05	3.911	−148.444	−0.06503(8)	5.62	12.20	49867.0	295	19.2	20.12	17.51	0.55
J1845−0434	B1842−04	6.163	−143.409	+0.2989(3)	5.83	11.90	49610.0	210	16.5	37.68	31.84	2.30
J1847−0402	B1844−04	1.673	−144.702	+0.08200(3)	5.26	12.75	49142.0	421	22.9	50.58	2.89	0.44
J1848−0123	B1845−01	1.516	−12.075	+0.05418(5)	6.30	12.27	50407.0	288	16.2	19.92	17.61	0.45
J1848−1414	—	3.358	−0.158	+0.0009(12)	8.53	10.82	51269.0	141	12.0	1.12	1.12	1.10
J1848−1952	B1845−19	0.232	−1.254	−0.00041(12)	6.47	13.01	50515.0	177	16.2	4.11	4.06	3.89
J1849−0636	B1846−06	0.689	−21.953	−0.00971(3)	5.70	12.92	49142.0	343	21.7	9.55	4.69	0.53
J1850+1335	B1848+13	2.894	−12.497	−0.01154(11)	6.56	11.86	50128.0	214	18.3	1.98	0.39	0.27
J1851+0418	B1848+04	3.513	−13.431	+0.2039(6)	6.62	11.75	50113.0	254	18.2	29.26	4.39	1.42
J1851+1259	—	0.830	−7.924	+0.20318(11)	6.22	12.58	50106.0	193	18.4	134.53	41.85	1.09
J1852+0031	B1849+00	0.459	−20.398	−0.0095(5)	5.55	13.17	49995.0	231	18.8	32.45	29.14	21.70
J1852−2610	—	2.973	−0.775	+0.0153(5)	7.78	11.24	51249.0	124	11.9	0.88	0.30	0.27
J1854+1050	B1852+10	1.745	−1.938	+0.011(4)	7.15	11.79	50869.0	266	14.2	11.45	11.32	10.93
J1854−1421	B1851−14	0.872	−3.166	−0.02349(10)	6.64	12.34	50313.0	193	17.3	11.52	4.55	0.71
J1856+0113	B1853+01	3.739	−2911.541	+25.6829(3)	4.31	12.88	50523.0	344	16.3	3043.03	140.80	18.41
J1857+0057	B1854+00	2.802	−0.429	−0.0040(8)	8.02	11.15	50097.0	136	18.5	2.56	2.45	2.34
J1857+0212	B1855+02	2.405	−232.901	+0.24472(8)	5.21	12.62	49945.0	279	18.8	65.35	8.69	0.31
J1857+0943	B1855+09	186.494	−0.620	−0.0016(5)	9.68	8.50	50027.0	447	18.7	0.04	0.04	0.04
J1900−2600	B1857−26	1.633	−0.546	−0.00382(5)	7.68	11.55	50105.0	228	18.2	1.13	0.31	0.22
J1901+0156	B1859+01	3.470	−28.379	−0.0225(7)	6.29	11.92	49345.0	131	11.6	1.03	0.86	0.31
J1901+0331	B1859+03	1.526	−17.358	+0.07654(7)	6.14	12.35	50312.0	252	17.3	54.54	51.24	1.33
J1901+0716	B1859+07	1.553	−5.498	+0.0571(3)	6.65	12.09	50016.0	364	18.9	133.31	130.51	9.78
J1901−0906	—	1.122	−1.032	+0.0013(3)	7.24	11.94	51277.0	140	12.0	0.41	0.36	0.34
J1902+0556	B1900+05	1.339	−23.098	+0.04707(8)	5.96	12.50	50112.0	354	18.2	18.75	2.26	0.61
J1902+0615	B1900+06	1.485	−16.990	−0.03224(8)	6.14	12.36	50300.0	401	17.2	9.12	3.42	0.60
J1903+0135	B1900+01	1.371	−7.582	−0.00650(4)	6.46	12.24	50430.0	242	16.3	2.96	2.20	0.37
J1903−0632	B1900−06	2.315	−18.224	+0.23973(11)	6.30	12.09	50430.0	215	16.3	61.75	40.77	0.58
J1904+0004	—	7.167	−6.065	+0.0410(8)	7.27	11.11	51269.0	147	12.0	1.80	1.44	0.45
J1904−1224	—	1.332	−1.317	−0.0035(8)	7.20	11.88	51037.0	95	8.9	0.52	0.50	0.47
J1905+0709	B1903+07	1.543	−11.750	+0.5539(3)	6.32	12.26	49856.0	355	19.6	266.65	81.60	8.82
J1905−0056	B1902−01	1.555	−7.378	−0.01931(8)	6.52	12.15	50127.0	220	18.3	5.93	1.19	0.26
J1906+0641	B1904+06	3.741	−29.895	−0.00358(10)	6.30	11.88	50016.0	246	18.9	0.98	0.78	0.31
J1907+4002	B1905+39	0.809	−0.354	−0.00010(6)	7.56	11.92	49144.0	364	23.7	2.28	2.29	2.20
J1909+0007	B1907+00	0.983	−5.336	+0.00586(3)	6.47	12.38	49121.0	328	22.8	21.37	19.16	0.73
J1909+0254	B1907+02	1.010	−5.634	+0.07290(12)	6.45	12.37	50496.0	264	16.3	27.55	2.09	0.74
J1909+1102	B1907+10	3.526	−32.811	−0.01965(5)	6.23	11.94	50316.0	379	17.3	13.65	13.66	0.33
J1910+0358	B1907+03	0.429	−0.822	+0.0283(4)	6.92	12.51	50428.0	193	16.1	31.57	15.22	4.44
J1910+1231	B1907+12	0.694	−3.959	+0.0006(3)	6.44	12.54	49275.0	173	22.8	2.50	2.31	2.18
J1910−0309	B1907−03	1.982	−8.593	−0.08667(14)	6.56	12.03	50430.0	186	16.3	21.56	12.27	1.99
J1911−1114	—	275.805	−1.065	+0.005(6)	9.61	8.36	51513.0	253	10.4	0.05	0.05	0.05
J1912+2104	B1910+20	0.448	−2.042	−0.00149(16)	6.54	12.68	50299.0	253	17.2	2.18	1.73	1.69
J1913+1400	B1911+13	1.918	−2.955	−0.01266(9)	7.01	11.82	50314.0	255	17.3	3.15	1.22	0.25

PSR J	PSR B	ν (s^{-1})	$\dot{\nu}$ ($10^{-15} s^{-2}$)	$\ddot{\nu}$ ($10^{-24} s^{-3}$)	$\log_{10}(\tau_c)$	$\log_{10} B_s$ (G)	Epoch (MJD)	N	T_{span} (yr)	σ_1 (ms)	σ_2 (ms)	σ_3 (ms)
J1913−0440	B1911−04	1.211	−5.963	+0.014721(3)	6.51	12.27	47036.0	543	35.0	53.91	13.14	0.79
J1915+1009	B1913+10	2.472	−93.191	+0.03947(6)	5.62	12.40	50389.0	454	16.8	7.78	4.05	0.32
J1915+1606	B1913+16	16.941	−2.476	+0.0036(7)	8.04	10.36	46444.0	346	18.3	0.47	0.46	0.38
J1915+1647	—	0.619	−0.155	+0.00050(9)	7.80	11.91	49290.0	256	22.8	2.70	2.64	2.53
J1916+0951	B1914+09	3.700	−34.482	−0.02010(12)	6.23	11.92	50312.0	291	17.3	2.64	1.44	0.25
J1916+1312	B1914+13	3.548	−46.027	−1.36038(10)	6.09	12.01	50312.0	310	17.3	172.41	64.62	5.03
J1917+1353	B1915+13	5.138	−189.997	+0.33352(3)	5.63	12.08	50161.0	517	18.1	33.63	10.90	0.48
J1917+2224	B1915+22	2.348	−15.798	+0.006(4)	6.37	12.05	51813.0	164	9.1	2.49	2.49	2.33
J1918+1444	B1916+14	0.847	−152.252	−0.08907(6)	4.95	13.20	50088.0	475	18.3	126.51	110.21	2.90
J1919+0021	B1917+00	0.786	−4.739	+0.00497(5)	6.42	12.50	49832.0	367	19.7	13.41	12.92	1.26
J1920+2650	B1918+26	1.273	−0.056	+0.00017(19)	8.56	11.22	50095.0	123	17.1	1.53	1.55	1.53
J1921+1419	B1919+14	1.618	−14.657	+0.02964(11)	6.24	12.27	48698.0	304	26.0	30.57	13.61	2.10
J1921+1948	B1918+19	1.218	−1.329	+0.00153(13)	7.16	11.94	48395.9	173	22.9	3.65	3.28	3.14
J1921+2153	B1919+21	0.748	−0.754	−0.000077(19)	7.20	12.13	48469.7	302	22.1	0.49	0.48	0.47
J1922+2018	B1920+20	0.853	−0.472	−0.0012(4)	7.46	11.95	50085.0	194	18.3	3.26	3.33	3.22
J1922+2110	B1920+21	0.928	−7.038	+0.03863(11)	6.32	12.48	50305.0	344	17.3	26.56	19.12	1.17
J1926+0431	B1923+04	0.931	−2.130	+0.01533(11)	6.84	12.22	50300.0	206	17.0	6.65	1.42	0.69
J1926+1434	B1924+14	0.755	−0.125	+0.00017(9)	7.98	11.74	49142.0	136	18.3	2.15	2.17	1.98
J1926+1648	B1924+16	1.725	−53.526	+0.01525(9)	5.71	12.51	50122.0	436	18.3	31.84	31.63	1.00
J1932+1059	B1929+10	4.415	−22.561	−0.0225058(18)	6.49	11.71	46926.0	768	35.7	49.34	44.61	0.43
J1932+2020	B1929+20	3.728	−58.625	−0.18479(11)	6.00	12.03	50302.0	224	17.2	21.29	5.44	0.74
J1932+2220	B1930+22	6.922	−2756.790	+40.6659(8)	4.60	12.47	51867.0	410	8.9	418.59	31.23	16.53
J1933+2421	B1931+24	1.229	−12.213	+0.63194(15)	6.20	12.41	51014.0	579	13.5	101.44	43.31	4.29
J1935+1616	B1933+16	2.788	−46.642	+0.0150133(11)	5.98	12.17	46827.0	936	36.2	28.89	4.97	0.27
J1937+2544	B1935+25	4.976	−15.917	−0.00337(10)	6.69	11.56	50126.0	370	18.3	0.51	0.46	0.20
J1939+2134	B1937+21	641.928	−43.314	+0.0179(8)	8.37	8.61	49389.0	517	22.2	0.04	0.03	0.03
J1939+2449	B1937+24	1.550	−43.904	+0.8292(6)	5.75	12.54	50351.0	128	12.4	123.97	100.22	6.20
J1941−2602	B1937−26	2.482	−5.892	−0.00806(7)	6.82	11.80	50498.0	193	16.3	1.31	0.18	0.11
J1943−1237	B1940−12	1.028	−1.751	+0.00034(3)	6.97	12.11	49145.0	138	23.7	1.23	1.14	0.49
J1944−1750	B1941−17	1.189	−1.394	+0.0097(3)	7.13	11.96	50314.0	139	17.3	4.87	3.12	2.06
J1945−0040	B1942−00	0.956	−0.489	−0.00004(8)	7.49	11.88	48532.0	141	27.0	1.91	1.92	1.87
J1946+1805	B1944+17	2.270	−0.124	+0.00035(6)	8.46	11.02	49291.0	240	22.8	0.98	0.97	0.95
J1946−2913	B1943−29	1.042	−1.617	−0.00139(6)	7.01	12.08	49123.0	117	22.8	1.79	0.84	0.75
J1948+3540	B1946+35	1.394	−13.723	+0.004243(14)	6.21	12.36	49852.0	458	19.8	3.82	3.01	0.22
J1949−2524	B1946−25	1.044	−3.566	−0.00057(6)	6.67	12.25	48533.0	128	22.9	1.42	1.18	0.54
J1952+1410	B1949+14	3.636	−1.694	+0.0009(13)	7.53	11.28	50096.0	141	16.0	1.72	1.71	1.59
J1952+3252	B1951+32	25.296	−3739.491	+17.1322(4)	5.03	11.69	50249.0	656	17.6	355.49	54.32	8.64
J1954+2923	B1952+29	2.344	−0.009	+0.00011(14)	9.59	10.44	49137.0	203	16.2	0.20	0.20	0.19
J1955+2908	B1953+29	163.048	−0.789	−0.0014(14)	9.51	8.64	49456.0	313	21.8	0.43	0.43	0.41
J1955+5059	B1953+50	1.927	−5.096	−0.009170(12)	6.78	11.93	49145.0	405	22.2	3.89	0.51	0.13
J1957+2831	—	3.250	−32.849	+0.0209(12)	6.20	12.00	51873.0	247	8.9	1.14	1.07	0.56
J2002+3217	B2000+32	1.435	−216.622	−0.87458(5)	5.02	12.94	50015.0	496	18.9	459.77	233.08	5.64
J2002+4050	B2000+40	1.105	−2.123	−0.00202(4)	6.92	12.10	50094.0	387	18.3	1.01	0.56	0.40
J2004+3137	B2002+31	0.474	−16.723	−0.011606(18)	5.65	13.10	49142.0	424	22.7	19.68	17.56	0.56
J2005−0020	—	0.877	−9.876	−0.0025(17)	6.15	12.59	51404.0	140	11.0	3.55	3.57	3.47
J2006−0807	B2003−08	1.722	−0.136	−0.0031(4)	8.30	11.22	50190.0	302	17.7	2.90	2.79	2.73
J2013+3845	B2011+38	4.344	−167.035	+0.01260(11)	5.61	12.16	50094.0	457	18.3	2.88	2.45	0.60
J2018+2839	B2016+28	1.792	−0.476	+0.004641(3)	7.78	11.46	46774.0	617	36.5	12.57	1.59	0.32
J2019+2425	—	254.160	−0.454	−0.028(8)	9.95	8.23	51351.0	169	11.0	0.09	0.09	0.09
J2022+5154	B2021+51	1.890	−10.939	−0.0182612(16)	6.44	12.11	47028.0	781	35.1	64.51	45.79	0.33
J2023+5037	B2022+50	2.684	−18.091	+0.04043(6)	6.37	11.99	50313.0	365	17.3	7.19	3.03	0.24
J2029+3744	B2027+37	0.822	−8.323	−0.06458(8)	6.19	12.59	50094.0	230	18.5	39.77	3.42	0.98
J2030+2228	B2028+22	1.586	−2.225	+0.0132(5)	7.05	11.88	51088.0	161	13.1	1.80	0.93	0.56
J2037+3621	B2035+36	1.616	−11.772	−0.48722(15)	6.34	12.23	50093.0	162	17.3	180.22	97.45	8.31
J2038+5319	B2036+53	0.702	−0.465	+0.0012(4)	7.38	12.07	50122.0	93	13.9	1.95	1.91	1.85
J2046+1540	B2044+15	0.879	−0.141	+0.00004(5)	8.00	11.66	49850.0	341	19.8	0.73	0.73	0.73
J2046+5708	B2045+56	2.098	−48.934	+0.0105(3)	5.83	12.37	50155.0	299	18.0	5.40	4.81	1.89
J2046−0421	B2043−04	0.646	−0.615	+0.00016(3)	7.22	12.18	49763.0	353	20.3	0.89	0.87	0.83
J2048−1616	B2045−16	0.510	−2.848	−0.0009500(16)	6.45	12.67	46827.0	594	36.1	12.82	7.58	0.52
J2051−0827	—	221.796	−0.626	+0.007(4)	9.75	8.38	51481.0	302	10.7	0.08	0.08	0.08
J2055+2209	B2053+21	1.227	−2.017	−0.00025(6)	6.98	12.02	50095.0	253	18.3	0.54	0.52	0.51
J2055+3630	B2053+36	4.515	−7.524	−0.01150(3)	6.98	11.46	49753.0	472	20.2	1.85	0.69	0.13
J2108+4441	B2106+44	2.410	−0.501	+0.00107(10)	7.88	11.28	50315.0	292	17.3	0.64	0.61	0.60
J2113+2754	B2110+27	0.831	−1.813	+0.000256(18)	6.86	12.25	49133.0	383	23.6	0.88	0.79	0.73
J2113+4644	B2111+46	0.986	−0.694	+0.017725(4)	7.35	11.94	47007.0	601	35.2	80.60	8.21	2.51
J2116+1414	B2113+14	2.272	−1.494	−0.00395(6)	7.38	11.56	49855.0	372	19.8	2.15	1.86	0.44
J2124+1407	B2122+13	1.441	−1.594	+0.0042(4)	7.16	11.87	50276.0	79	17.2	1.55	0.74	0.73
J2124−3358	—	202.794	−0.846	+0.011(5)	9.58	8.51	51284.0	226	11.7	0.08	0.08	0.08
J2145−0750	—	62.296	−0.115	−0.0006(3)	9.93	8.84	51173.0	469	12.3	0.02	0.02	0.02
J2149+6329	B2148+63	2.631	−1.177	−0.00136(4)	7.55	11.41	49852.0	388	19.8	0.67	0.56	0.26
J2150+5247	B2148+52	3.010	−91.574	−0.02643(5)	5.72	12.27	50094.0	400	18.3	5.74	3.42	0.31
J2155−3118	B2152−31	0.971	−1.169	+0.0023(3)	7.12	12.06	50429.0	124	16.3	2.05	1.82	1.77
J2157+4017	B2154+40	0.656	−1.477	−0.03803(3)	6.85	12.36	49686.0	473	20.5	45.25	8.30	1.01
J2212+2933	B2210+29	0.995	−0.491	−0.00270(15)	7.51	11.85	50093.0	303	18.3	1.65	1.19	1.13
J2219+4754	B2217+47	1.857	−9.537	−0.002956(3)	6.49	12.09	46471.0	509	35.2	7.50	2.61	0.65
J2222+2923	—	3.554	−0.078	+0.0018(16)	8.86	10.62	51671.0	231	9.9	0.96	0.95	0.95
J2225+6535	B2224+65	1.465	−20.734	+0.01545(7)	6.05	12.41	49142.0	516	23.7	18.41	16.35	0.84
J2229+2643	—	335.816	−0.171	−0.005(7)	10.49	7.83	51625.0	249	9.8	0.03	0.03	0.03
J2229+6205	B2227+61	2.257	−11.489	−0.01031(16)	6.49	12.00	50081.0	214	17.5	3.05	2.38	0.47
J2242+6950	B2241+69	0.601	−1.741	−0.0003(3)	6.74	12.46	50092.0	114	18.5	3.30	3.28	3.08
J2248−0101	—	2.095	−2.894	+0.0351(4)	7.06	11.75	51270.0	171	12.0	3.15	0.81	0.52
J2257+5909	B2255+58	2.716	−42.428	−0.10513(4)	6.01	12.17	50502.0	236	16.1	16.40	5.92	0.57
J2305+3100	B2303+30	0.635	−1.164	−0.00143(6)	6.94	12.33	50302.0	277	17.3	1.42	1.04	0.74
J2305+4707	B2303+46	0.938	−0.500	−0.0008(4)	7.47	11.90	50088.0	185	17.3	4.50	4.47	4.35
J2308+5547	B2306+55	2.105	−0.884	−0.00535(7)	7.58	11.49	49841.0	394	19.7	2.01	0.87	0.52
J2313+4253	B2310+42	2.862	−0.920	+0.006386(7)	7.69	11.30	48202.7	498	25.6	3.59	0.87	0.13
J2317+1439	—	290.255	−0.204	−0.001(8)	10.35	7.97	51656.0	202	9.8	0.04	0.04	0.04
J2317+2149	B2315+21	0.692	−0.502	−0.00009(4)	7.34	12.10	49142.0	300	20.2	0.55	0.54	0.54
J2321+6024	B2319+60	0.443	−1.382	−0.00122(3)	6.71	12.61	49332.0	347	22.6	2.89	1.39	1.12
J2322+2057	—	207.968	−0.418	+0.004(9)	9.90	8.34	51335.0	150	11.4	0.08	0.08	0.07

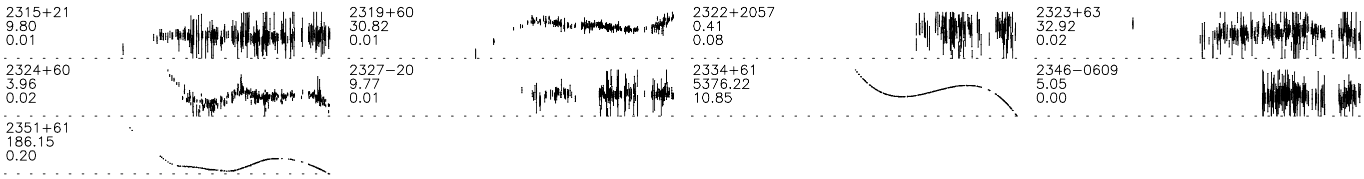

Figure 1. . . . continued

PSR J	PSR B	ν (s^{-1})	$\dot{\nu}$ ($10^{-15} s^{-2}$)	$\ddot{\nu}$ ($10^{-24} s^{-3}$)	$\log_{10}(\tau_c)$	$\log_{10} B_s$ (G)	Epoch (MJD)	N	T_{span} (yr)	σ_1 (ms)	σ_2 (ms)	σ_3 (ms)
J2325+6316	B2323+63	0.696	−1.370	+0.00053(7)	6.91	12.31	48714.0	381	26.1	4.57	4.44	4.38
J2326+6113	B2324+60	4.280	−6.458	+0.00222(4)	7.02	11.46	50069.0	394	18.3	0.51	0.46	0.28
J2330−2005	B2327−20	0.608	−1.714	−0.00003(7)	6.75	12.45	50304.0	231	16.2	1.11	1.11	1.08
J2337+6151	B2334+61	2.019	−781.495	+3.12568(14)	4.61	12.99	50094.0	464	18.3	862.99	4.44	1.20
J2346−0609	—	0.846	−0.977	−0.0014(4)	7.14	12.11	51426.0	236	11.2	0.63	0.60	0.59
J2354+6155	B2351+61	1.058	−18.219	+0.023876(17)	5.96	12.60	49276.0	375	22.8	23.27	6.72	0.52

3 DISCUSSION

The large-scale structures seen in the timing residuals of these pulsars are not due to the observing systems or offline processing. Some of these pulsars are also observed as part of long-term timing programs at other observatories; in all cases we see the same large-scale features in the timing residuals. The structures are also not being produced by the off-line processing. We have obtained timing residuals from site-arrival-times using three pulsar timing packages, PSRTIME, TEMPO and TEMPO2 for many of our pulsars. Again, we see the same features in all cases. Finally, the choice of clock corrections applied to the data and the exact choice of solar system ephemeris can be shown not to be causing the observed timing noise.

3.1 Dispersion measure variations

It has been postulated that the effects of interstellar or interplanetary dispersion measure (DM) variations may lead to timing noise. The large-scale structures seen in our data are observed at all observing frequencies and so are not due to DM variations. For instance, we show in Figure **??**, the timing residuals for PSR B1815−14 at 20 cm overlaid with other frequencies. It is likely that smaller scale variations will be due to DM effects. The interplanetary DM variations are mainly due to the solar wind. This is modelled to sufficient precision within TEMPO2. The millisecond pulsar PSR J1022+1001 has the smallest ecliptic latitude in our sample of -0.06°. However, this pulsar is not observed when the line-of-sight to the pulsar is close the Sun and so the extra DM delay expected is insignificant. Only for J1730−2304 do we see a significant variation (Figure 3). However, the variation is small, restricted in time to a few days per year and is well modelled in TEMPO2.

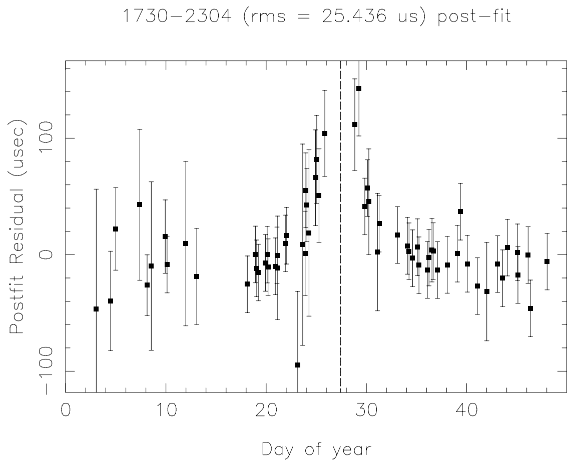

Figure 3. Timing residuals for PSR J1730−2304 without fitting for the solar wind. The vertical dotted line represents the closest approach of the line-of-sight to the Sun.

3.2 Categorising the timing noise

It is instructive to categorise the pulsars by the structures seen in their timing residuals. As the TOAs for some pulsars are measured much more precisely than others any such scheme can only be approximate. For instance, in Figure 4 we plot the detailed structure observed for PSR B1900+01 overlaid on the residuals for PSR B1745−20 that are seemingly flat. It is also unfortunate that for the frequently glitching pulsars it often impossible to obtain a timing solution over a long observation span. The short spans that are available do not clearly show the variety of structures present in their timing residuals.

However, very broadly the pulsars can be classified into A) flat residuals, B) cubics corresponding to $\ddot{\nu} > 0$, C) cubics where $\ddot{\nu} < 0$ and D) curves that are more complicated than cubics. Examples of each classification are given in Figure 5. 37% of our sample are characterised as type A pulsars, 24% as type B, 22% as type C and 17% as type D. However, it is important to emphasise that the classification of any particular pulsar is likely to change as more data are obtained. For instance, in Figure 6 we plot the timing residuals that would have been obtained for PSR B0950+08 if we had access only to a) one, b) five, c) six, d) eleven and e) 35-years of observations. With these data it is likely that the pulsar would have been classified as type A, C, B and E respectively.

3.3 The cubics

For those pulsars whose residuals are dominated by a cubic term (and hence are denoted as type 'B' or 'C') we plot, in Figure 7, the timing residuals after the cubic term has been removed. The recycled pulsars PSR B1620−26 and

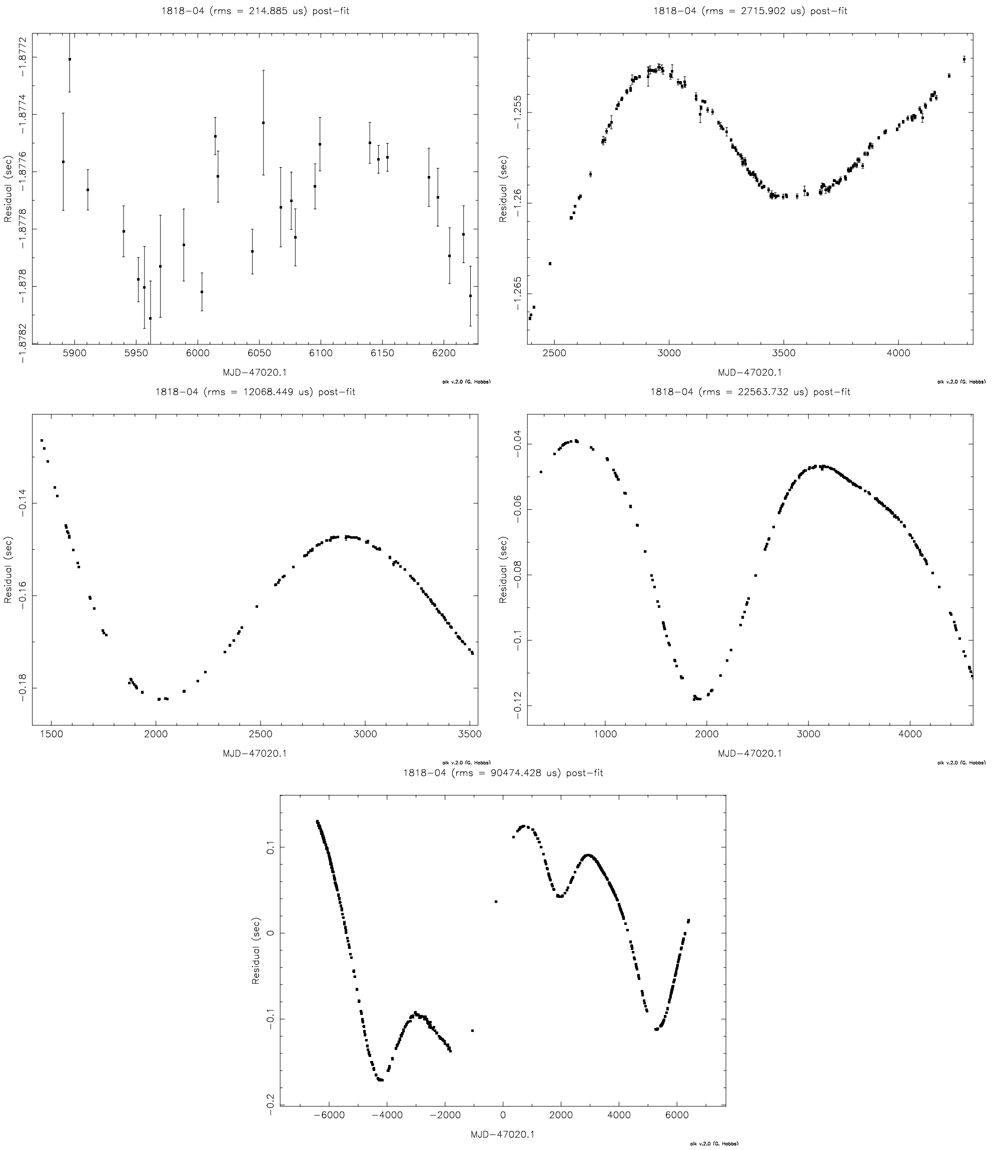

Figure 6. The timing residuals for PSR B0950+08 obtained from different sections of the entire data span available. In each section the pulsar's spin-frequency and its first derivative have been fitted. The data spans are approximately a) 1 year, b) 5 years, c) 6 years, d) 11 years and e) the full 35 years.

B1820−30A are unusual in that they are the only millisecond pulsars that are not characterised by an 'A' indicating flat residuals. The timing residuals for both of these pulsars are dominated by a cubic term of type 'B'. They both lie within globular clusters (M4 and NGC6624 respectively) and the cubic terms are therefore explained as being due to the acceleration of the pulsar in the cluster's gravitational field.

A pulsar's measured braking index can be calculated from

$$n = \frac{\nu\ddot{\nu}}{\dot{\nu}^2} \tag{1}$$

where a value of $n = 3$ is predicted for a pulsar slowing down due to pure magnetic dipole radiation. However, the measured braking indices for the non-recycled pulsars range from −287986 to +36246 with a mean of −1713 and median of 22. For the pulsars with data spanning more than 30 years we obtain braking indices ranging from −1701 to +36246 with a mean of +3750 and median +29.

Clearly for $n = 3$ the $\ddot{\nu}$ value will be positive as

$$\ddot{\nu}_{dipole} = 3\dot{\nu}^2/\nu \tag{2}$$

Out of our sample of 126 pulsars, 68 (54%) have a postive measure $\ddot{\nu}$ value and 46% with negative $\ddot{\nu}$. As concluded, in Paper I, the $\ddot{\nu}$ values are clealy not due to magnetic dipole radiation.

Six of our pulsars have reported glitch events. For these, three have positive $\ddot{\nu}$ and three have negative $\ddot{\nu}$.

For the 19 pulsars in our sample where we have more than 30 years of timing data we show, in Figure 8 measured $\ddot{\nu}$ values obtained using different data spans and over different sections of the data. For these 19 pulsars, only six have negative $\ddot{\nu}$ when measured over the entire data span. Those pulsars with positive $\ddot{\nu}$ have corresponding braking indices

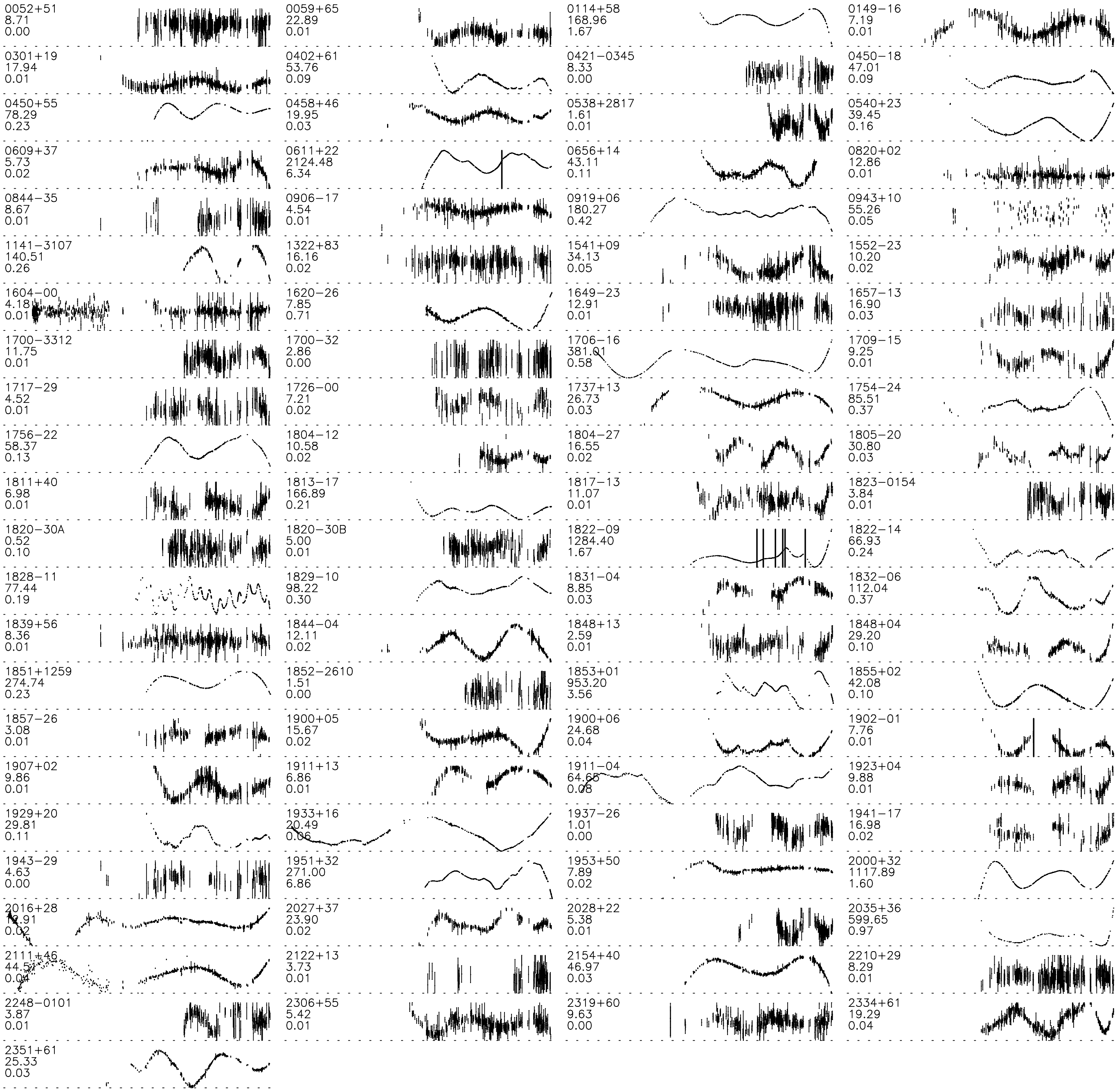

Figure 7. Pulsar timing residuals after the removal of a cubic term

of 70, 24, 1126, 35, 94, 2592, 30, 144, 510, 19, 36448 and 36878. **what are errors in these numbers?**

Glitch events prior to the first observation will produce cubics where $\ddot{\nu} > 0$ (ie. pulsars of type B). In Figure 9 we plot $|\ddot{\nu}|$ versus the pulsars' characteristic ages τ_c. Pulsars with $\ddot{\nu} > 0$ are indicated with 'plus' symbols and those with $\ddot{\nu} < 0$ with circles. For the youngest pulsars, with $\tau_c < 10^5$ all except one pulsar has $\ddot{\nu} > 0$ which is explainable by the timing noise for young pulsars being dominated by the recovery from glitch events. Almost equal numbers of the older pulsars exist with the different signs of $\ddot{\nu}$.

can we show that the youngest pulsars are all dominated by the recovery from glitches whereas all older pulsars are dominated by pseudo-sinusoidal timing residuals?

We note that long-term timing noise is not dominated by cubic terms - ie. the total number of pulsars characterised as type B or C for 10 yr dataspans is 40%,for 15 yr dataspans 50%, for 20 yr dataspans 53% and for 25 yr spans 57%. **something wrong here**.

3.4 Stability

For each pulsar we calculate various stability parameters which are listed in Table XXX. We include the Δ_8 value introduced by Arzoumanian et al. (1994):

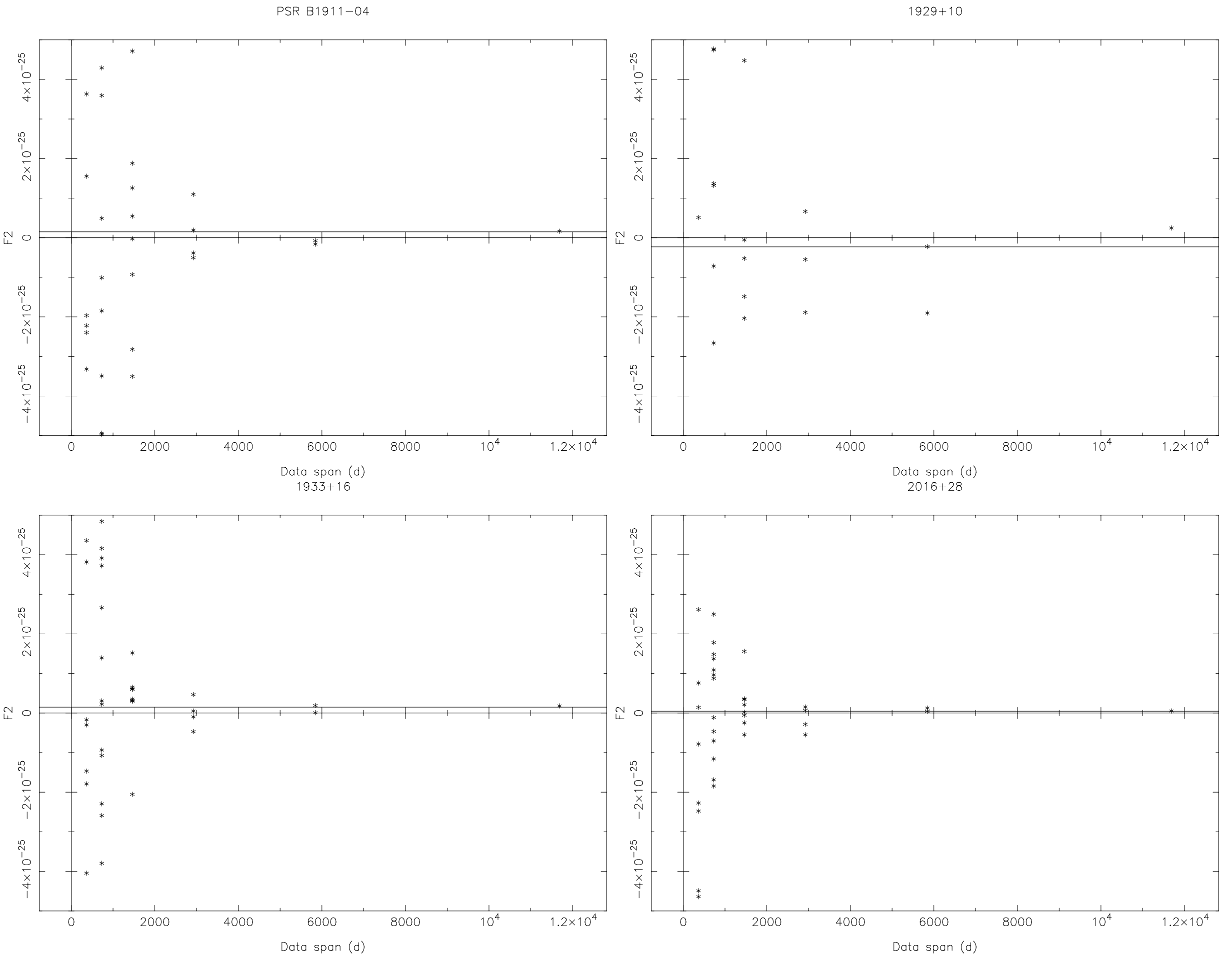

Figure 8. Frequency second derivative values obtained using different dataspans of 1, 2, 4, 8, 16 and 32 years.

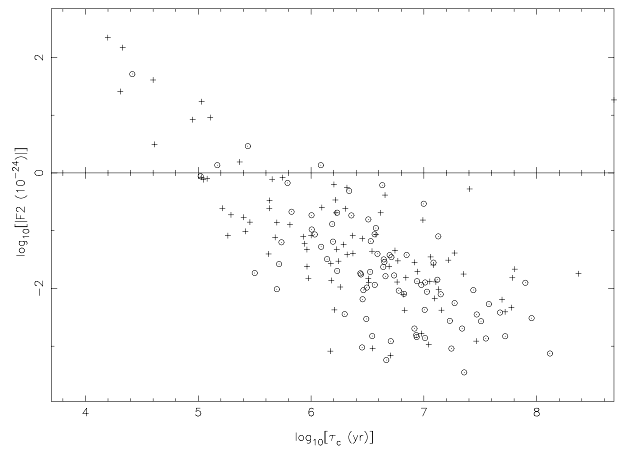

Figure 9. $\ddot{\nu}$ vs τ_c.

.

$$\Delta_8 = \log_{10}\left(\frac{1}{6\nu}|\ddot{\nu}|t^3\right) \quad (3)$$

where the spin-frequency, ν and its second derivative, $\ddot{\nu}$, are measured over a $t = 10^8$ sec ($\sim$ 3.16 yr) interval. As our pulsar data-sets contain at least 10 yr of data, we list the average Δ_8 value and its variance obtained by fitting for ν and $\ddot{\nu}$ in unique 3 yr segments.

The Δ_8 parameter provides information at only one specified time-scale. More recently, Matsakis, Taylor & Eubanks (1997) showed how the σ_z parameter can be applied to pulsar timing residuals where

$$\sigma_z(\tau) = \frac{\tau^2}{2\sqrt{5}}\langle c^2\rangle^{1/2} \quad (4)$$

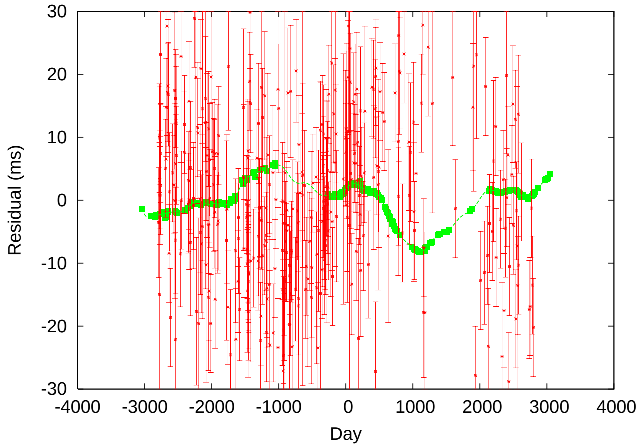

Figure 4. The timing residuals for PSR B1900+01 (thick, line) overlaid on the timing residuals for PSR B1745−20.

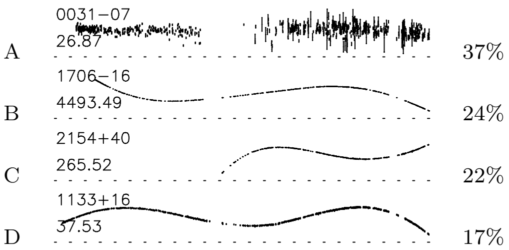

Figure 5. A classification scheme for structures seen in the timing residuals. The pulsars shown are a) PSR B0031−07, b) B1706−16, c) B2154+40 and d) B1133+16.

where the magnitude, c, of cubic terms fitted to short sections of the dataspan, τ are averaged to give. In Figure 10 we plot the $\sigma_z(\tau)$ parameter for pulsars within given characteristic age ranges. For comparison we include the σ_z curve for the publically available Arecibo observatory observations of PSR B1855+09 (Kaspi et al. 1994), a comparison between the two time-scales NIST and PTB (Edwards, private communication) and the expected stability limit due to a gravitational wave background. To produce a statistic for comparison with other pulsar parameters we record, in Table 3, the σ_z parameter measured at $\tau = 3\,$yr and also at $\tau = 10\,$yr.

In Figure XXX we compare the following stability measures: $\ddot{\nu}$, Δ_8, $\sigma_z(3\text{yr})$, $\sigma_z(10\text{yr})$. In Figure XXX we plot $\sigma_z(10\text{yr})$ versus the pulsars' spin-frequency, frequency-derivative, characteristic age, surface magnetic field, energy loss rate and magnetic field at the light cylinder.

3.5 Power spectra

For each of our pulsars we obtain a Lomb-Scargle periodogram after whitening the timing residuals using multiple frequency-derivative terms. We also obtain a power-spectrum obtained from the amplitude of fitted Gram-Schmidt polynomials to the non-whitened data-sets.

We list, in Table 2, any significant periodicities found in the Lomb-Scargle periodograms.

We represent each Gram-Schmidt spectrum as $P(f) = Af^\alpha$ and record the amplitude and power-law index α in Table 3.

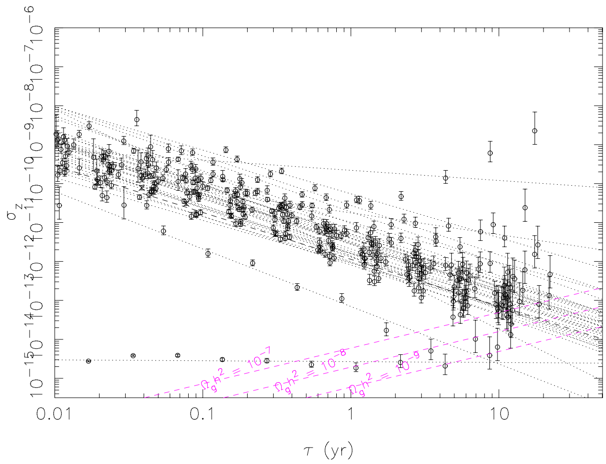

Figure 10. σ_z parameter versus timescale, τ for the recycled pulsars.

Table 2. Periodicities found in the recycled pulsar residuals

PSR	Period (d)	Period (yr)	Prob.
J0621+1002	582.62	1.60	1.93×10^{-15}
B1620−26	187.81	0.51	3.90×10^{-4}
B1937+21	51.43	0.14	3.54×10^{-4}
	68.08	0.19	$\sim 3 \times 10^{-4}$

Note: B1620−26 requires significant whitening. The periodicity observed may be part of the "red"-noise. The periodicity is also close to the known orbital period of 191 d.

ACKNOWLEDGEMENTS

During the course of this work we made extensive use of NASA's Astrophysics Data System bibliographic database and the astro-ph preprint service.

REFERENCES

Kaspi V. M., Taylor J. H., Ryba M., 1994, ApJ, 428, 713
Matsakis D. N., Taylor J. H., Eubanks T. M., 1997, AA, 326, 924

Table 3. Table of offsets and gradients in the power spectra

PSR	σ_z(3yr)	σ_z(10yr)	offset	gradient
0034-0534			-0.21 ± 0.13	0.01 ± 0.07
0218+4232			-0.14 ± 0.14	0.09 ± 0.08
0613-0200			-3.35 ± 0.55	-1.47 ± 0.22
0621+1002			-0.63 ± 0.30	-0.39 ± 0.15
0751+1807			-0.60 ± 0.13	-0.26 ± 0.07
1012+5307			-0.24 ± 0.20	-0.08 ± 0.10
1022+1001			-1.49 ± 0.30	-0.74 ± 0.15
1024-0719			-0.27 ± 0.19	-0.03 ± 0.10
1300+1240			0.33 ± 0.25	0.26 ± 0.12
1455-3330			-0.80 ± 0.41	-0.26 ± 0.17
1518+4904			-0.24 ± 0.18	-0.01 ± 0.09
1537+1155			-0.28 ± 0.16	-0.14 ± 0.08
1623-2631			-6.21 ± 1.06	-2.34 ± 0.36
1643-1224			-2.10 ± 0.48	-0.89 ± 0.20
1713+0747			-1.00 ± 0.44	-0.43 ± 0.18
1730-2304			-2.11 ± 0.46	-0.91 ± 0.17
1744-1134			-0.85 ± 0.55	-0.38 ± 0.21
1804-0735			-1.23 ± 0.25	-0.42 ± 0.11
1804-2717			-0.88 ± 0.48	-0.35 ± 0.19
1823-3021A			-6.14 ± 1.06	-2.26 ± 0.36
1824-2452			-3.63 ± 0.77	-1.33 ± 0.28
1857+0943			-1.66 ± 0.30	-0.70 ± 0.12
1911-1114			-0.09 ± 0.20	-0.01 ± 0.10
1915+1606			-1.87 ± 0.30	-0.70 ± 0.11
1939+2134			-1.52 ± 0.30	-0.80 ± 0.12
1955+2908			0.43 ± 0.42	0.22 ± 0.16
2019+2425			1.04 ± 0.51	0.58 ± 0.21
2051-0827			-0.17 ± 0.14	-0.04 ± 0.07
2124-3358			-0.28 ± 0.19	-0.06 ± 0.09
2145-0750			-1.11 ± 0.34	-0.47 ± 0.15
2229+2643			-0.57 ± 0.25	-0.12 ± 0.12
2317+1439			1.34 ± 0.55	0.65 ± 0.23
2322+2057			-0.77 ± 0.44	-0.12 ± 0.18